

# Visual Properties of Neurons in Area V4 of the Macaque: Sensitivity to Stimulus Form

ROBERT DESIMONE AND STANLEY J. SCHEIN

*Laboratory of Neuropsychology, National Institute of Mental Health, and  
National Eye Institute, National Institutes of Health, Bethesda, Maryland 20892;  
and Howe Laboratory, Harvard Medical School, Massachusetts Eye and Ear Infirmary,  
Boston, Massachusetts 02114*

## SUMMARY AND CONCLUSIONS

1. Area V4, a visuotopically organized area in prestriate cortex of the macaque, is the major source of visual input to the inferior temporal cortex, known to be crucial for object recognition. To examine the selectivity of cells in V4 for stimulus form, we quantitatively measured the responses of 322 cells to bars varying in length, width, orientation, and polarity of contrast, and sinusoidal gratings varying in spatial frequency, phase, orientation, and overall size. All of the cells recorded in V4 were located on the lower portion of the prelunate gyrus.

2. Receptive fields were located almost exclusively within the representation of the central 5° of the lower visual field, and receptive field size, in linear dimension, was 4–7 times greater than that in the corresponding representation of striate cortex (V1). Nearly all receptive fields consisted of overlapping dark and light zones, like “classic” complex fields in V1, but the relative strengths of the dark and light zones often differed. A few cells responded exclusively to light or dark stimuli.

3. Many cells in V4 were selective for stimulus orientation, and a few were selective for direction of motion as well. Although the median orientation bandwidth of the orientation-selective cells (52°) was wider than that reported for oriented cells in V1, ~8% of the oriented cells had bandwidths of <30°, which is nearly as narrow as the most narrowly tuned cells in V1. The proportion of cells selective for direction of motion (13%) was not markedly different from that reported in V1.

4. The large majority of V4 cells were tuned to the length and width of bars, and the “shape” of the optimal bar varied from cell to cell, as has been reported for cells in the dorsolateral visual area (DL) of the owl monkey, a possible homologue of V4 in the macaque. Preferred lengths and widths varied independently from ~0.05 to 6°, with the smallest preferred bars about the size of the smallest receptive fields in V1 and the largest preferred bars larger than any fields in V1. The relationship between the size of the optimal bar and the size of the receptive field varied from cell to cell. Some cells, for example, responded best to bars much narrower or shorter than the field, whereas other cells responded best to bars that filled (but did not extend beyond) the excitatory field in the length, width, or both dimensions. These variations in the size of the optimal stimulus can be explained in terms of two underlying receptive-field mechanisms, the balance between summation and antagonism within the receptive field and the strength of “silent” suppressive zones beyond the excitatory receptive field.

5. Cells in V4 were also tuned to the spatial frequency of sinusoidal gratings. Optimal frequencies spanned a range of at least six octaves, from 0.12 to 8 cycles per degree (cpd), which was the full range tested. As with preferred bar size, the relationship between the optimal spatial frequency and the width of the receptive field varied greatly from cell to cell. At one extreme, some cells showed a high degree of spatial summation within the receptive field, responding best to gratings that covered the receptive field with a single half-cycle. In

terms of spatial summation, these cells most resembled simple, or linear, cells in V1, and, as with simple cells, the width of their excitatory receptive fields could often be predicted from the Fourier transform of their spatial frequency response function. Furthermore, some cells exhibiting both high summation and a strong preference for light or dark within their excitatory field showed nearly the same degree of phase sensitivity as simple cells. At the other extreme, some cells showed antagonism to continuous regions of light or dark in the field, responding best to gratings that filled the receptive field with many narrow bars. These cells most resembled complex, or nonlinear, cells in V1, and, as with complex cells, the width of their excitatory receptive fields was much wider than predicted from the Fourier transform of their spatial frequency response function.

6. For most V4 cells, the closer the overall size of the gratings was to the dimensions of the receptive field, the larger was the response. These results add to the evidence provided by bar length and width tuning for silent suppressive mechanisms beyond the classically defined receptive fields of V4 cells.

7. A few cells in V4 that responded poorly or not at all to sine-wave gratings were found to respond well to bars and square-wave gratings, suggesting that edge sharpness may be explicitly represented in V4.

8. Our finding that most cells in V4 are highly selective for stimulus form, in conjunction with the finding that most cells in V4 are selective for wavelength, establishes that both form and color are processed together within V4, as is true of V1, V2, and the inferior temporal cortex. These physiological findings, together with the results of behavioral and anatomical studies, support the notion that V1, V2, V4, and the inferior temporal cortex constitute a hierarchical system mediating the perception and recognition of objects.

## INTRODUCTION

In primates, the corticocortical pathway from striate cortex, or V1, through prestriate cortex into the inferior temporal cortex appears to play a critical role in the ability to recognize objects by sight (14, 68). Though neuronal properties plausibly useful for object recognition have been described at both the

early (V1) and late (inferior temporal) stages of this occipitotemporal system, little is known about such properties in the intervening prestriate areas. We therefore began exploring neuronal properties in area V4, a visuotopically organized area that receives visual inputs from V1 by way of areas V2 and V3 (21, 22, 68, 73) and is the major source of visual input to the inferior temporal cortex (11).

Prior neurophysiological studies of V4 have focused primarily on the color properties of the cells, beginning with Zeki's (74-79) original reports that V4 was specialized almost exclusively for the analysis of color. More recently, several groups have reported that most V4 cells are not highly selective for color, which has left the status of V4 in question (9, 23, 37, 55, 70). In a series of three studies, we have examined quantitatively both the spectral and spatial properties of V4 cells. In this first study, the goal was to understand how variations in the spatial structure of stimuli influence the responses of the cells.

A wide variety of stimuli were used to probe the spatial selectivity of the cells, including bars varying in length, width, orientation, and polarity of contrast (black/white), and sinusoidal gratings varying in spatial frequency, phase, orientation, and overall size. The results showed that most V4 cells are highly sensitive to stimulus form, and that the selectivity of V4 cells for such features as length, width, orientation, and spatial frequency is comparable with that reported for cells in V1 and V2. Some cells in V4 have properties that resemble those of simple cells in V1, some have properties that resemble those of complex cells, and some have properties not previously described in V1. The responses of a given V4 cell appear to be determined by the balance between summation and antagonism within its receptive field as well as by the strength of "silent" suppressive zones beyond the classically defined receptive field.

In a companion study, we have found that the large majority of V4 cells respond to white light but also carry information about wavelength (54; and in preparation). These results, in conjunction with the results of the present study, argue for multidimensional processing of visual information within V4, as has been found in V1, V2, and inferior temporal cortex, the other primary constituents of the occipitotemporal pathway (14).

## METHODS

### *Animal preparation*

Seven monkeys (*Macaca fascicularis*), weighing 2.5–4.5 kg, were used. Two weeks prior to the first recording session, the monkey was anesthetized with sodium pentobarbital, and a recording chamber and bolt for holding the head were affixed to the skull using aseptic techniques. The bone underlying the recording chamber was left intact. To determine the approximate location of the prelunate gyrus within the chamber, we removed a 2-cm disk of bone from the opposite hemisphere, and visualized the lunate, superior temporal and inferior occipital sulci. In most cases, the sulci could be seen through the exposed dura mater, but in a few cases it was necessary to open the dura. The stereotaxic coordinates of the prelunate gyrus were recorded, and the bone opening was covered with a stainless steel cap. Based on these coordinates, the boundaries of the gyrus were drawn on a thin layer of acrylic covering the bone inside the recording chamber of the opposite hemisphere. Subsequent histology indicated that this technique for localizing the prelunate gyrus was accurate within 2–3 mm.

### *Recording procedure*

The recording procedure has been described in detail by Desimone and Gross (12). Briefly, the animal was anesthetized with halothane (2.5%) in a mixture of nitrous oxide and oxygen (50:50) and intubated with an endotracheial tube coated with a local anesthesia (lidocaine). Following placement of the animal's head in a stereotaxic frame (using the previously implanted bolt to hold the head), a small (1–2 mm) burr hole was drilled in the bone over the prelunate gyrus. The monkey was then paralyzed with pancuronium bromide and anesthetized for the remainder of the recording session with a mixture of nitrous oxide and oxygen (70:30). The eye contralateral to the recording chamber was treated with cyclopentolate and was focused at 57 or 114 cm with a contact lens. The electrocardiograph (EKG) was continuously monitored for signs of pain reactions, and end-tidal CO<sub>2</sub> and body temperature were maintained within normal physiological limits. The recording sessions generally lasted 8–12 h. At the end of the session, the recording chamber was filled with antibiotic (2% tetracycline) and capped, and the infusion of the paralytic was terminated. When the monkey was breathing normally, it was returned to its cage. At least 1 wk intervened between successive recording sessions, and each monkey was used in 1–20 sessions.

Typically, a single electrode penetration was made through the burr hole in the skull in each recording session, and the same hole was used for three or four sessions. The recording electrodes were made of varnish-coated tungsten with exposed tips

of 10–15  $\mu\text{m}$ . Electrodes were advanced in the horizontal plane toward the prelunate gyrus (see Fig. 1). Since the electrodes were never advanced more than 2 mm through the surface cortex or through the white matter underlying the surface cortex, we were assured that all recordings were confined to the cortex on the surface of the gyrus and the most superficial portions of the adjacent banks (i.e., area V4) and did not extend into neighboring visual areas, such as V3, V3A, and the middle temporal area (MT), located deep in the banks of the lunate and superior temporal sulci. Because of the long survival times of most of our animals and the short lengths of the electrode penetrations, it was not possible to recover most of the individual electrode tracks. Therefore, to facilitate histological localization, we made long electrode penetrations through the centers of the burr holes at the completion of recording in each animal. On the following day the monkey was given an overdose of sodium pentobarbital and perfused intracardially with Formol-saline. The brain was removed, blocked, photographed, sectioned at 30  $\mu\text{m}$ , and stained for cells (thionine) and myelin (25) (see Fig. 1). Examination of the stained sections confirmed that the electrode tracts were all located in the cortex of the prelunate gyrus.

### *Stimuli*

Stimuli were presented on either a rear-projection screen or cathode-ray tube (CRT) screen, and a mirror was used to switch between the two. The rear-projection screen was used primarily for presenting stimuli of different wavelengths and is to be described in a separate report. The CRT in the initial experiments was a Joyce Electronics display with a white (P4) phosphor. The display was located 57 cm from the animal's eye, its size was adjusted to be 10  $\times$  10°, its mean luminance was 7.6 ft-L, and its refresh rate was 100 Hz. The magnetic deflection plates of the display were mounted on a servomotor-driven assembly, and their orientation was controlled by an analog signal from a computer (PDP-11). The Z-input to the display was also controlled by the computer, allowing the production of one-dimensional luminance modulated patterns such as gratings and bars of any orientation. In later experiments, the CRT was a high-speed color graphics display monitor (Conrac 7211). The monitor was located 114 cm from the animal's eye, its size was 10  $\times$  14°, and its mean luminance was 12 ft-L. The monitor was mounted inside a set of metal rings riding on roller bearings and could be rotated easily. A Jupiter-7+ graphics controller, linked by a direct-memory-access (DMA) interface to the computer, generated stimuli on the screen. The graphics controller displayed 483 horizontal by 640 vertical lines on the screen with a full-screen refresh rate of 60 Hz, twice the standard television rate. The graphics

memory was 8 bits deep, allowing 256 different shades of gray or colors on the screen at one time. Each 8-bit display memory value was used as an index into a 24-bit lookup table that set the actual red, green, and blue outputs. The relationship between the outputs of the controller and the luminance of stimuli on the display was checked with a photometer and was found to be nonlinear. To compensate, the lookup table values were adjusted to provide a linear relationship between values in the graphics memory and the luminance of the screen. The graphics system could display two-dimensional patterns of arbitrary shape, orientation, luminance profile, and color. Stimuli could be turned on and off by setting a bit in a read mask during the vertical flyback interval. Bars were swept across the screen at 1–2°/s with a hardware pan feature of the graphics system, whereas gratings were drifted by shifting values in the lookup table during the flyback interval. For quantitative grating experiments, the orientation of the gratings was set by physical rotation of the monitor, so that the bars in the grating always ran along the vertical lines of the display raster. The stimuli on both the black-and-white and the color graphic displays could be controlled either by the computer, for quantitative experiments, or manually (with joysticks and dials), for qualitative mapping of receptive fields and the initial exploration of cell properties.

The contrast of gratings was defined using the Michaelson formula

$$\text{contrast} = (L_{\max} - L_{\min}) / (L_{\max} + L_{\min})$$

where  $L$  is luminance. The contrast of bars was defined as the luminance difference between the bar and the background divided by the background luminance. For both bars and gratings, the contrast was set at 50%.

#### *Experimental design*

For each cell encountered, we first tried to map its receptive field with dark, light, or colored bars swept across the screen under manual control. While mapping the receptive field, we also noted any specificity of the cell for orientation, color, length, or width. Quantitative tests of the cell's spectral or spatial properties were then conducted by varying one stimulus dimension (such as length) at a time, holding all other stimulus qualities constant at the optimal value for the cell. In the initial experiments, the spectral properties were generally studied first, and, if the cell was maintained, the spatial properties second, whereas in later studies this order was reversed. Quantitative tests of spatial selectivity were normally conducted with a white or black stimulus unless a cell strongly preferred a particular color.

For the quantitative studies, the responses to visual stimuli were compiled into conventional averaged response histograms. Because the responses

of V4 cells in the anesthetized preparation may vary considerably over time, all of the stimuli we wished to compare were presented in randomly interleaved order until at least ten trials had accumulated for each. The interval between the end of one trial and the beginning of the next was 2–5 s. In experiments with drifting gratings, the temporal frequency was fixed at 1 Hz, and the gratings were on for 5 s/trial. All responses were computed by subtraction of the average activity during the prestimulus interval from that during the stimulation interval, and thus represented the average change in activity produced by the stimulus. For experiments with moving bars, we also calculated the peak response, which was the maximal firing rate during any 100-ms (typical) interval.

#### **RESULTS**

A total of 332 neurons were studied in seven animals. The approximate locations of all recording sites are shown in Fig. 1. All sites were located on the prelunate gyrus, within the "V4-complex" of Zeki (75), "area V4" of Ungerleider et al. (68) and Gattass et al. (26), and "area V4-AL" of Maguire and Baizer (41).

#### *Size and location of receptive fields*

Of the cells encountered, 93% (305/332) responded to visual stimuli. Consistent with the visual topography that has been described in V4 (26, 65, 68), the receptive-field centers of nearly all cells (298/305) were located within the representation of the central 5° of the lower contralateral quadrant of the visual field. The few exceptions had receptive fields located between 6 and 19° from the fovea in the lower visual field. To avoid comparisons among cells with very different receptive field eccentricities, we confine all further descriptions to the cells whose receptive-field centers were located within the representation of the central 5° of the visual field.

Receptive fields generally had a central "hot zone" of maximal responsiveness, which diminished progressively with distance from the center. We took the size of the receptive field to be the largest cumulative region from which light, dark, or colored bars could reliably elicit excitatory responses, as judged either by ear or by computer mapping. Receptive-field size (square root of area) as a function of eccentricity ( $e$ ) is shown in Fig. 2. The equation for the regression line is

$$\text{RF size} = 0.66 + 0.42 e \quad (r = 0.63)$$

The line relating receptive-field size to eccen-

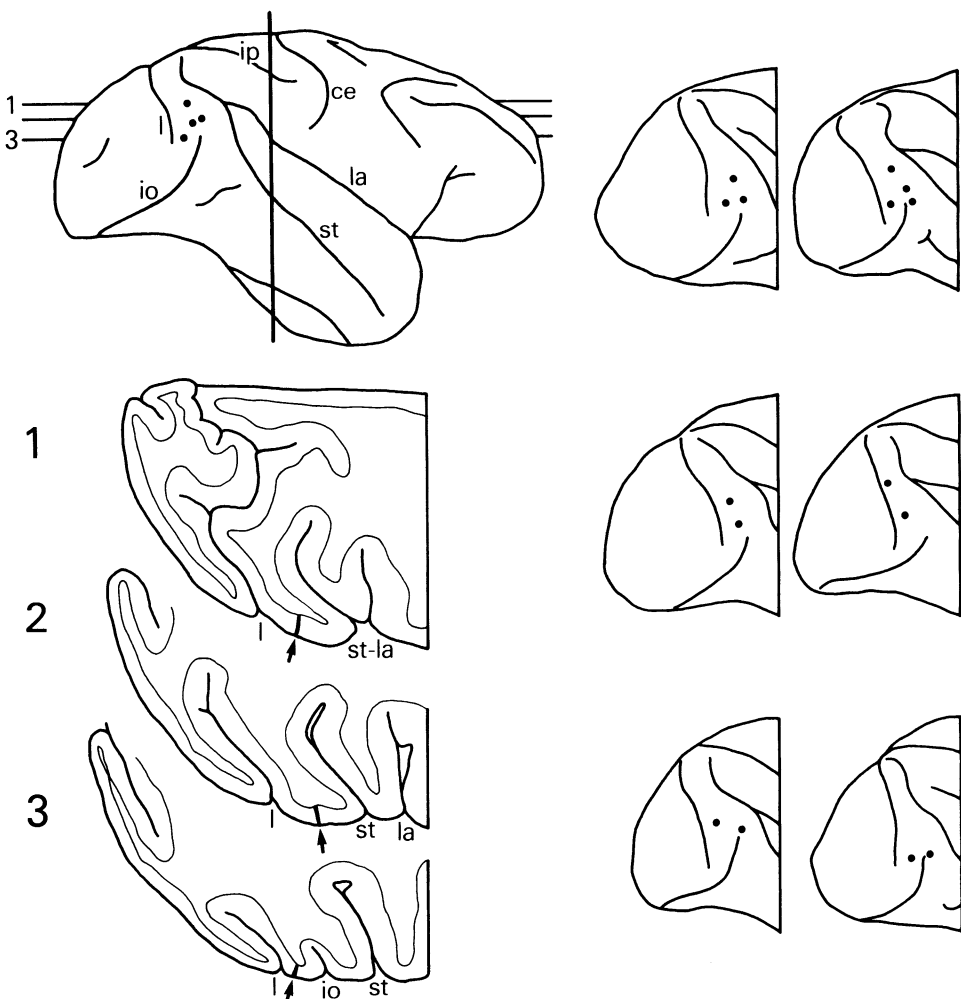


FIG. 1. Recording sites in the 7 monkeys. Each dot on the 7 hemispheres marks the center of a 1- to 2-mm recording zone in which 3–4 penetrations (typically) were made. Representative horizontal sections from one of the hemispheres are shown on the bottom left. Reconstructed tracts (heavy lines) in the prelunate gyrus are indicated by arrows. In all animals, the penetrations were confined to the portion of V4 located on the surface of the prelunate gyrus and the most superficial portions of the adjacent banks. Abbreviations: ce, central sulcus; ip, intraparietal sulcus; io, inferior occipital sulcus; l, lunate sulcus; la, lateral sulcus; st, superior temporal sulcus.

tricity in V1 (20, 35) is shown for comparison. At an eccentricity of 1°, V4 receptive fields are approximately four times larger than V1 fields in linear dimension, or 16 times larger in area. At an eccentricity of 5° they are approximately seven times larger in linear dimension or ~50 times larger in area. Thus the properties of cells in V4 must ultimately derive from many cells in V1.

#### *Experiments with bars*

**RECEPTIVE-FIELD MAPS.** From the manual mapping of receptive fields it appeared that if a V4 cell responded at all to both light and

dark bars, the light and dark response zones were coextensive or nearly so. In this respect, the receptive fields resembled those of complex cells in V1 (33, 35, 56). To check these qualitative findings, the responses of 36 cells were measured quantitatively to light and dark bars presented at several locations (typically 7 or 8) across their hand-mapped fields. Consistent with the qualitative mapping, the receptive fields of all cells that responded to light and dark bars had at least partially overlapping light and dark response zones. Examples of three such receptive fields are shown in Fig. 3. For most cells, like the one illustrated in

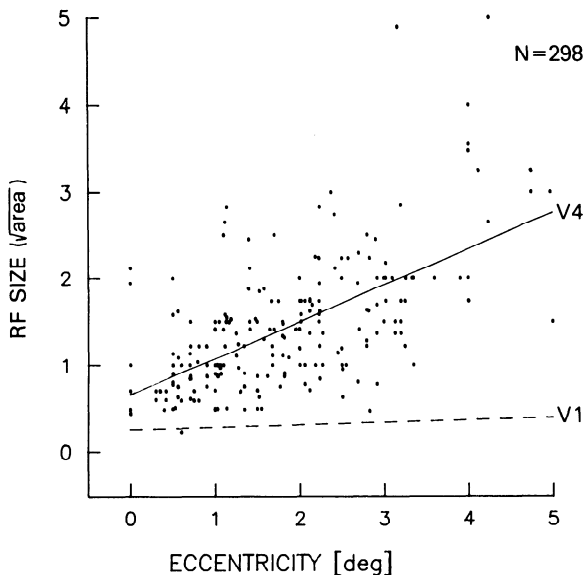


FIG. 2. Receptive-field (RF) size as a function of eccentricity within V4. The regression line relating size and eccentricity in V1 (20, 36) is shown for comparison.

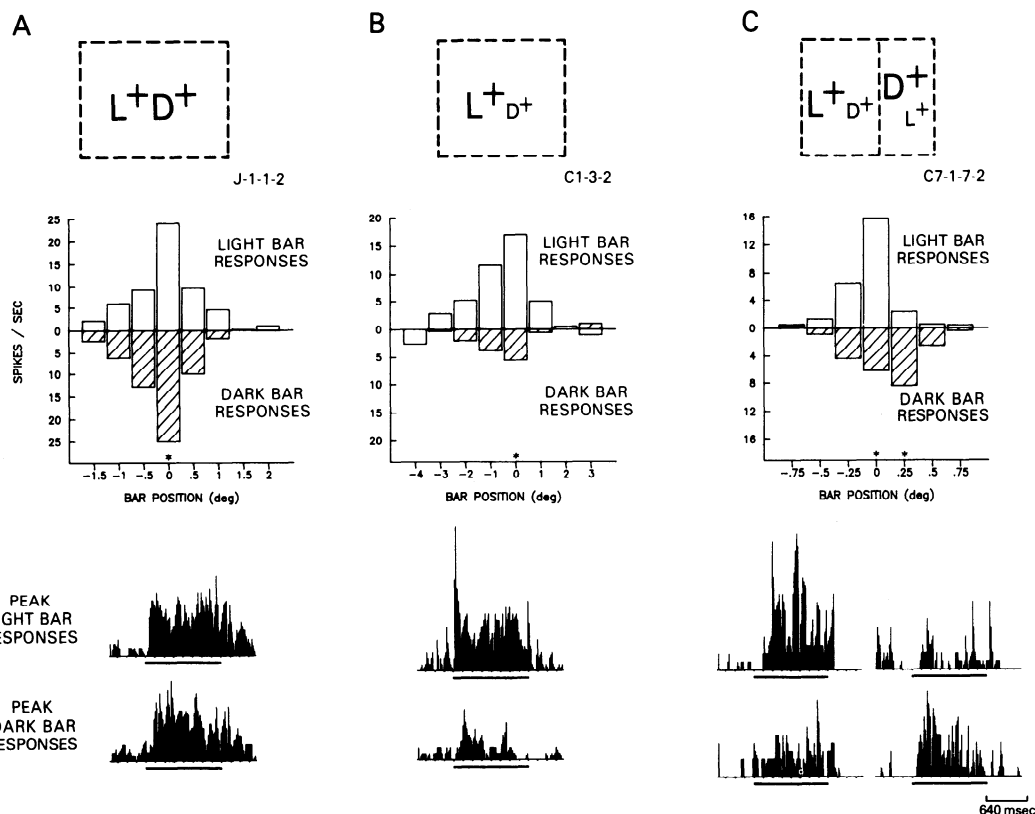


FIG. 3. Receptive fields of 3 cells in V4. For each of the 3 cells, light and dark bars were flashed at several locations within the hand-mapped receptive field. Excitatory responses to light bars are shown above the "0" line and to dark bars below. The reverse is true of inhibitory responses. The response histograms show the best responses to light and dark bars, at the locations indicated by the asterisks on the receptive-field plots.

Fig. 3A, the light and dark response zones were coextensive, but for a few (9/36) cells, like the one illustrated in Fig. 3C, the peaks of the light and dark zones were slightly offset. Some cells, such as the one in Fig. 3A, responded about equally to light and dark bars, but many cells, such as the one in Fig. 3B, showed a preference for light or dark or, in the extreme case, responded exclusively to light or dark (see Fig. 16).

One unexpected characteristic of most V4 cells was that their sensitivity to dark or light was evident only from their response to stimulus onset (e.g., see Fig. 3). Of the 36 cells with quantitatively mapped fields, only 4 gave any significant response to the offset of light or dark bars. For a few cells, OFF responses could be elicited at high light intensities, but at these intensities the experimenters typically experienced afterimages when viewing the stimuli. Thus, unlike the case for most cells in the retina, lateral geniculate, and possibly striate cortex, responses to the offset of light bars do not provide a good measure of the sensitivity of V4 cells to dark stimuli, and responses to the offset of dark bars do not provide a good measure of the sensitivity of V4 cells to light stimuli.

Because the light and dark bar response zones of V4 receptive fields often differed in either strength or precise location, we adopted a quantitative measure of such differences that had been developed by Dean and Tolhurst (8) to classify cells as simple or complex in the cat. At each location  $i$ , the excitatory response to the light bar was  $\text{light}(i)$ , a positive number, and the excitatory response to the dark bar was  $\text{dark}(i)$ , a negative number. (The sign of inhibitory responses was opposite to that of excitatory.) The light-dark difference index [termed by Dean and Tolhurst (8) a "discreteness" index] was then defined as

$$\text{difference index} = \frac{\sum |(\text{light}(i) + \text{dark}(i))|}{\sum |\text{light}(i)| + \sum |\text{dark}(i)|}$$

As described by Dean and Tolhurst (8), the difference index ranges from 0.0, when the dark and light bar responses are equivalent at every tested location, up to 1.0, when no location elicits both a light bar and dark bar excitatory response. A "classic" simple cell in V1, with nonoverlapping subfields, would have an index of 1.0 and a classic complex cell in V1, with coextensive and equal subfields,

would have an index of 0.0 (e.g., see Fig. 3A, index = 0.05). Intermediate values could be achieved either by cells with subfields that overlapped only partially (e.g., Fig. 3C, index = 0.50) or by cells with subfields that were coextensive but unequal in strength (e.g., Fig. 3B, index = 0.55).

The distribution of the difference index is shown in Fig. 4. Nearly all cells had intermediate values (i.e., neither 1.0 nor 0.0), which was due primarily to cells whose receptive fields contained overlapping dark and light zones that were unequal in strength. In the extreme case, cells responded exclusively to light or dark bars, which accounts for the few cells with indexes >0.9. Thus, although the receptive fields of V4 cells do not have separate light and dark subfields like those of classic simple cells in V1, information about whether a stimulus is light or dark is not lost in V4.

For two cells that did not respond to light or dark bars on a white background, we were able to map their receptive fields on a colored background using bars formed by increments (light bar) or decrements (dark bar) of the background color on the color-CRT screen. One of the cells was selective for green bars and the other for yellow. Both cells responded to both dark and light bars of the appropriate color, and the dark and light response zones were superimposed (but unequal in strength), similar to the behavior of V4 cells that responded to increments and decrements of white light.

**ORIENTATION AND DIRECTION SPECIFICITY.** Many cells in V4 exhibited orientation or direction selectivity. Orientation tuning bandwidths were measured quantitatively for 67 cells with moving bars and for 10 additional cells with moving gratings. Since the results from the two types of stimuli were very similar, we have pooled the results in all analyses. The stimuli used were at least 5° in length (i.e., generally two to three times the length of the receptive field) unless a receptive field was very strongly end stopped, in which case the stimuli were restricted to the length of the field. Stimuli were moved across the receptive field in directions that varied in 22.5°, or, occasionally, 10° steps. Tuning curves were drawn using linear interpolation, and the full width of the curve (about the peak) at half maximum response was taken to be the orientation

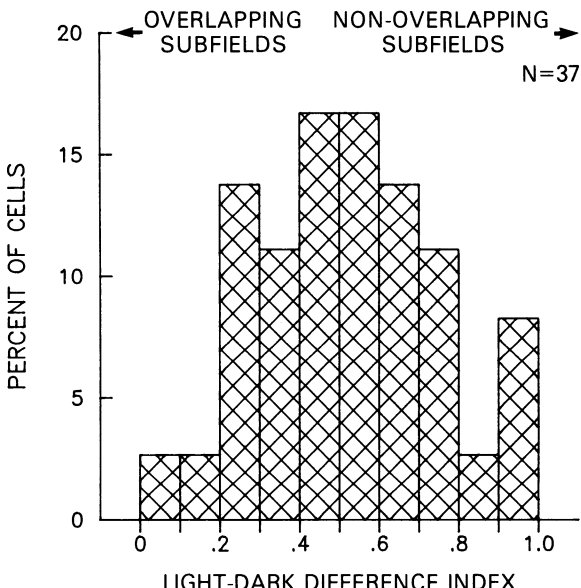


FIG. 4. A measure of the inequality of light and dark zones of receptive fields in V4. See text for the definition of the index. Cells whose receptive fields have coextensive and equal light and dark zones (e.g., a "classic" complex cell) have an index of 0.0, whereas cells whose receptive fields have nonoverlapping zones (e.g., a classic simple cell) or only a single zone have an index of 1.0.

bandwidth. Typical tuning curves are illustrated in Fig. 5.

As demonstrated in Fig. 6A, the distribution of orientation bandwidths in V4 is very broad, ranging from narrowly tuned cells with bandwidths  $<30^\circ$  (5.2% of the cells) to cells with little or no orientation tuning at all (e.g., bandwidths  $>90^\circ$ , 32.5% of the cells). Since the distribution of bandwidths in V4 covers nearly the same range as that reported for cells in V1 (16, 57), information about stimulus orientation appears to be maintained in V4. On the average, however, V4 cells are more likely to be broadly tuned or unoriented than are cells in V1. The median orientation bandwidth for all cells in V4 was  $74.5^\circ$ , and for oriented cells alone (i.e., excluding cells with bandwidths  $>90^\circ$ ) it was  $52^\circ$ , compared with  $42$  and  $37^\circ$ , respectively, in V1 (16; but see 57).

An index for direction-of-motion specificity (DS) was derived for the 77 cells that were studied with the full range of moving bars or gratings and for an additional 37 cells that were studied with a bar moving in either of two opposite directions at the optimal orientation. The index was calculated according to the following formula

DS = response to null direction/  
response to best direction

A cell without DS would have an index of 1.0, whereas a highly directional cell would have an index of 0.0 (or less if it was inhibited in the null direction). For a number of cells, the two best opposed directions were actually separated by  $157.5$  or  $202.5^\circ$  rather than  $180^\circ$ . Since this apparent shift of  $22.5^\circ$  from the expected  $180^\circ$  may have been due to discrete sampling in  $22.5^\circ$  steps, for these cells we calculated the DS index on the basis of the best direction and the one  $180 \pm 22.5^\circ$  opposite.

The distribution of the directionality index is shown in Fig. 6B. The distribution is highly skewed toward 1.0, i.e., an absence of directionality, yet there is a significant group of clearly directional cells. For example, 13% of the cells show more than a 10:3 response ratio (indexes  $<0.3$ ) to opposite directions of motion, which is not markedly different from the proportion of cells with an equivalent degree of directionality in V1 (1, 16, 19, 56). Thus, like V1, V4 does not appear to be particularly specialized for analyzing direction of motion but nonetheless has a population of directionally selective cells.

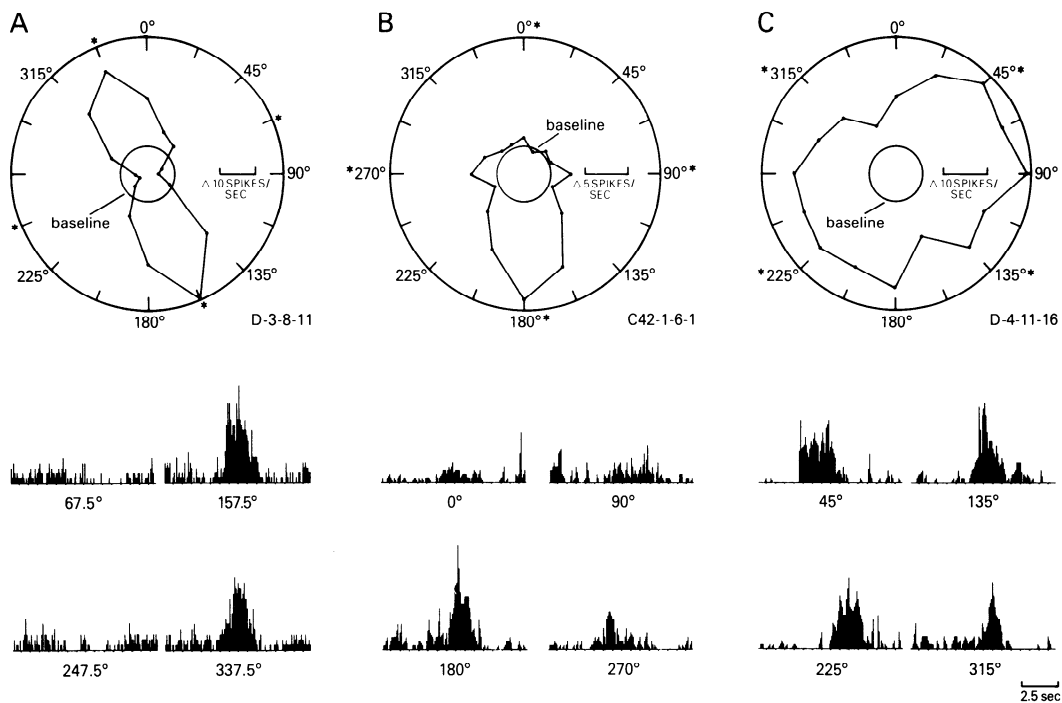


FIG. 5. Orientation tuning curves of 3 cells in V4. On the polar plots, the *inner circle* represents the base-line activity of the cell, and the *curve* shows the change in firing rate from base line at each orientation. The histograms under each of the *curves* show responses to bars swept at  $2^{\circ}/\text{sec}$  across the receptive field in the 4 directions indicated by the asterisks. The bars used in *A* were black, in *B*, green, and in *C*, white.

**SELECTIVITY FOR LENGTH AND WIDTH.** Both qualitative and quantitative testing showed that V4 cells were tuned to the length and

width of bars within the receptive field. Nearly all cells were tested with bars swept across the receptive field, and some were tested with bars

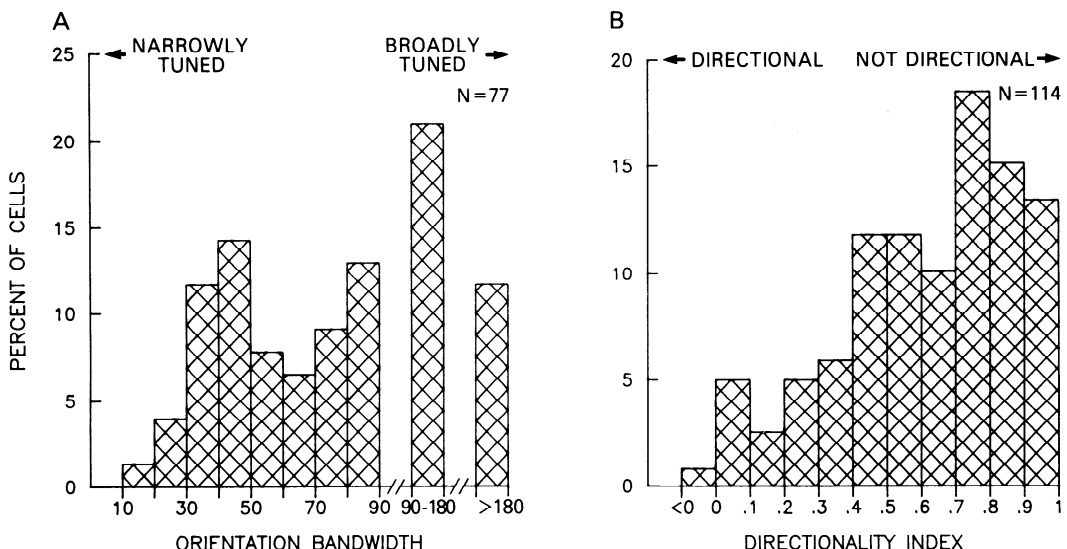


FIG. 6. Distribution of orientation bandwidths (*A*) and directionality indexes (*B*) in V4. The directionality index is the response in the null direction divided by the response in the best direction.

flashed within the field as well. For oriented cells, the dimensions of the bar corresponding to length and width were defined by the preferred orientation axis, i.e., length was parallel to the preferred orientation and width was orthogonal to it. For unoriented cells, the definitions of length and width were fixed by the axis of whatever stimulus motion was used. Length corresponded to the dimension orthogonal to the axis of motion and width to the dimension parallel to the axis of motion.

Typically, as the length or width of a bar was increased from some small value, the response of a V4 cell would increase until the length or width reached some critical dimension beyond which responses would begin to decrease. We shall refer to the bar with these critical dimensions as the "optimal" bar, with the qualification that the dimensions of the optimal bar might vary with testing conditions. Typical length and width tuning curves and optimal bars derived from the peaks of the curves are illustrated for four cells in Fig. 7. Cells in V4 differed from one another in several important respects. First, they varied in the absolute dimensions of their optimal bar. Second, they varied in the relationship between the size of the optimal bar and the size of the receptive field. Third, they varied in the shape and steepness of their tuning curves. Fourth, they varied in their relative response to moving versus flashed bars of different widths. All of these variations may be explained in terms of variations in two underlying receptive-field mechanisms, the balance between summation and antagonism within the receptive field and the strength of silent suppressive zones beyond the excitatory receptive field.

**Length.** A total of 52 cells were tested quantitatively with bars varying in length from (typically) 0.1–9°. All of the cells were tested with moving bars and 10 were tested with flashed bars as well. Optimal bar lengths ranged from 0.1 to 6°.

As can be seen from the length tuning curves of the two cells illustrated in Fig. 7, *B* and *D*, the responses of some V4 cells increased with stimulus length up to about the dimensions of the receptive field, beyond which responses were diminished sharply. Thus, these cells exhibited summation along the length axis within the receptive field and suppression beyond the receptive field, similar to the char-

acteristics of hypercomplex or end-stopped cells in V1 (35, 56). For many of the cells, responses were least to bars 9° in length (the maximum length tested), suggesting that the combined length of the excitatory receptive field and suppressive field was at least 9°. The suppressive zones were silent in that stimulation of these zones alone did not normally elicit either excitatory or inhibitory responses.

Other V4 cells, such as the ones illustrated in Fig. 7, *A* and *C*, responded best to short bars anywhere within a large excitatory receptive field, i.e., they exhibited antagonism along the length axis inside the field. We use the term antagonism in this context (rather than "suppression") because the reduction in response results from extension of a stimulus into portions of the field that are excitatory when stimulated alone. We reserve the term suppression for the reduction in response that occurs from extension of a stimulus into regions that do not elicit excitatory responses when stimulated alone. The responses of one of the cells (Fig. 7C) showed length summation for bars up to one-half the length of the receptive field and antagonism for longer bars, whereas the responses of the other cell (Fig. 7A) were best to practically the shortest bar tested. To our knowledge, cells with such properties have not been reported in V1 of monkeys, although they may exist in V1 of cats (27, 48) and area V2 of monkeys (5, 32; see DISCUSSION). A further interesting feature of these V4 cells was that their poor response to a long bar inside the field was reduced even further if the bar extended beyond the receptive field into the surround. Thus, both classes of cells, those with (Fig. 7, *A* and *C*) and those without (Fig. 7, *B* and *D*) antagonistic interactions for length within the receptive field, could exhibit additional length suppression from the surround. The balance between summation and antagonism within the field and the strength of the suppression from beyond the field appeared to determine the particular form of the length tuning curve of any given cell.

To quantify the selectivity for bar length, we calculated two indexes for each cell. The first, the length suppression index, was calculated as follows

length suppression

= response to longest bar tested/response to optimal bar

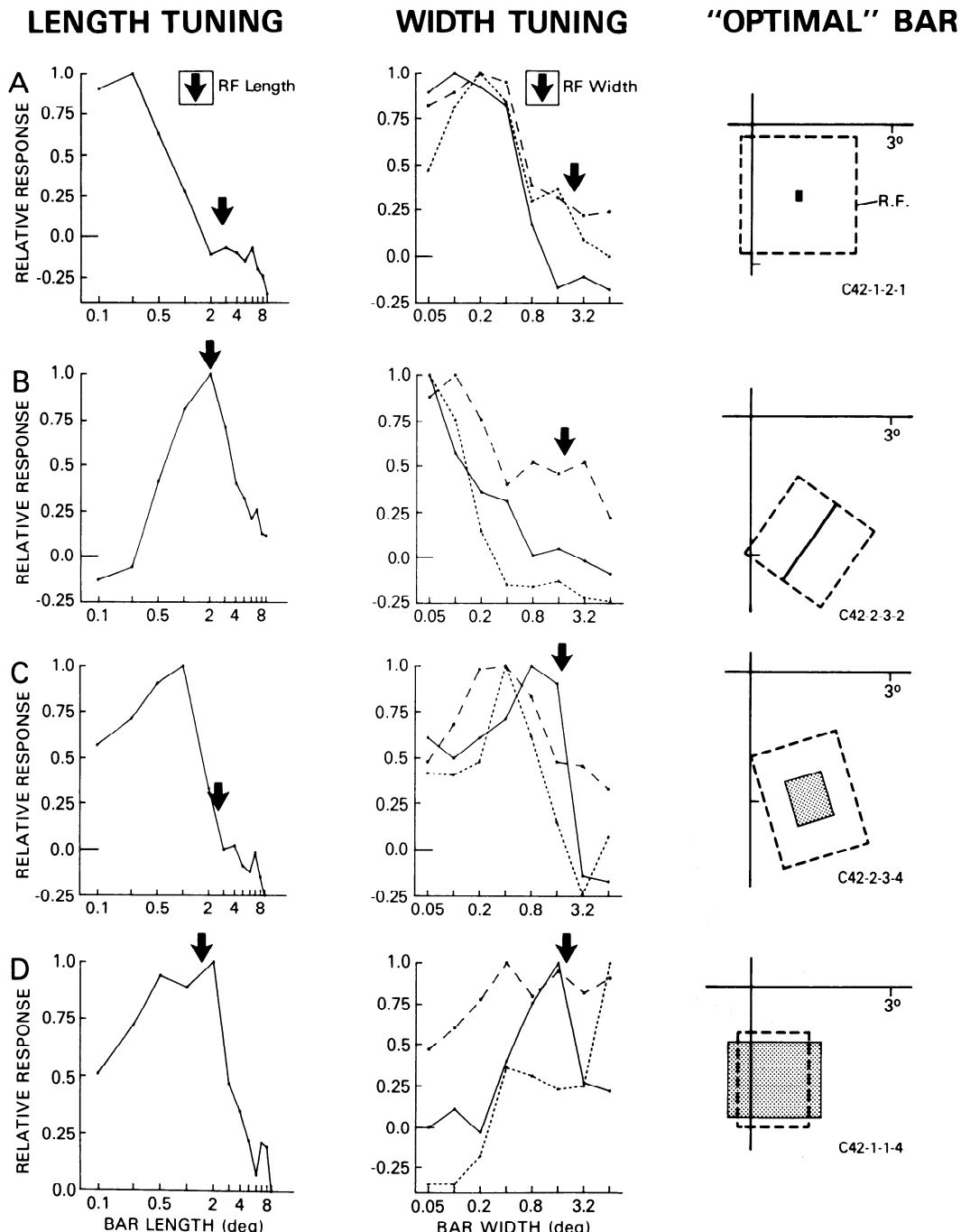


FIG. 7. Length and width tuning curves for 4 cells in V4. The length tuning curves were derived from the average firing rate to bars swept across the receptive field at 2°/s. The arrow on each curve indicates the length of the receptive field. The width tuning curves shown with solid lines are derived from the average firing rate to bars flashed within the receptive field for 128 ms. The width tuning curves shown with dotted bars or with dashed bars are derived from the average or peak response, respectively, to bars swept across the receptive field at 2°/s. The arrows indicate the width of the receptive field. The cell in *A* was studied with black bars, the cells in *B* and *C* with green bars, and the cell in *D* with white bars. For all curves, the maximal response has been normalized to 1.0 on the vertical axis, with 0.0 representing the spontaneous (prestimulus) firing rate. The length and width of the "optimal" bar shown to the right of each set of curves are taken from the peak of the length tuning curve and the peak of the width tuning curve for flashed bars.

This index reflects the strength of the mechanisms that reduce the response to long bars. The index would equal 1.0 for cells that showed no reduction of response to the longest bar tested (typically 9° but, in a few cases, 6.4°) compared with the response to the optimal bar and would equal 0.0 for cells that did not respond at all to the longest bar. As demonstrated by the distribution of the index in Fig. 8A, the responses of most cells were highly suppressed by long bars (indexes near 0.0), indicating a strong suppressive mechanism. In fact, for 44% of the cells the long bar actually reduced their activity below the spontaneous rate (index <0.0). For only a few cells was the response to the longest bar tested optimal or nearly optimal.

The second index used to quantify length selectivity was a length summation index, calculated as follows

length summation

= length of optimal bar/length of receptive field

The magnitude of this index is determined both by the degree of length summation within the receptive field and by the location of any length antagonistic or suppressive mechanism. Low index values indicate a low degree of

summation, and, in particular, values much smaller than 1.0 suggest that length antagonistic mechanisms operate within the receptive field. High index values indicate a high degree of length summation, with values near 1.0 or larger suggesting the absence of any antagonistic mechanism inside the field (without ruling out suppression from beyond the field).

As demonstrated in Fig. 8B, the relationship between the length of the optimal bar and the length of the receptive field varied widely across cells. For some cells, the length of the optimal bar was <10% of the length of the receptive field (index <0.1), whereas for other cells the best length was more than 150% the length of the field (index >1.5, see below). For 59% of the cells, the length of the optimal bar was clearly shorter than the length of the receptive field (indexes <0.9), indicating that most cells had antagonistic mechanisms inside the field. Nearly all of these cells exhibited further reductions in response to bars longer than the receptive field, indicating the existence of a length suppressive mechanism operating outside the receptive field in addition to the length antagonistic mechanism operating inside the field (e.g., Fig. 7, A and C). By contrast, for 41% of the cells the best stimulus was the length of the receptive field or longer. Three-

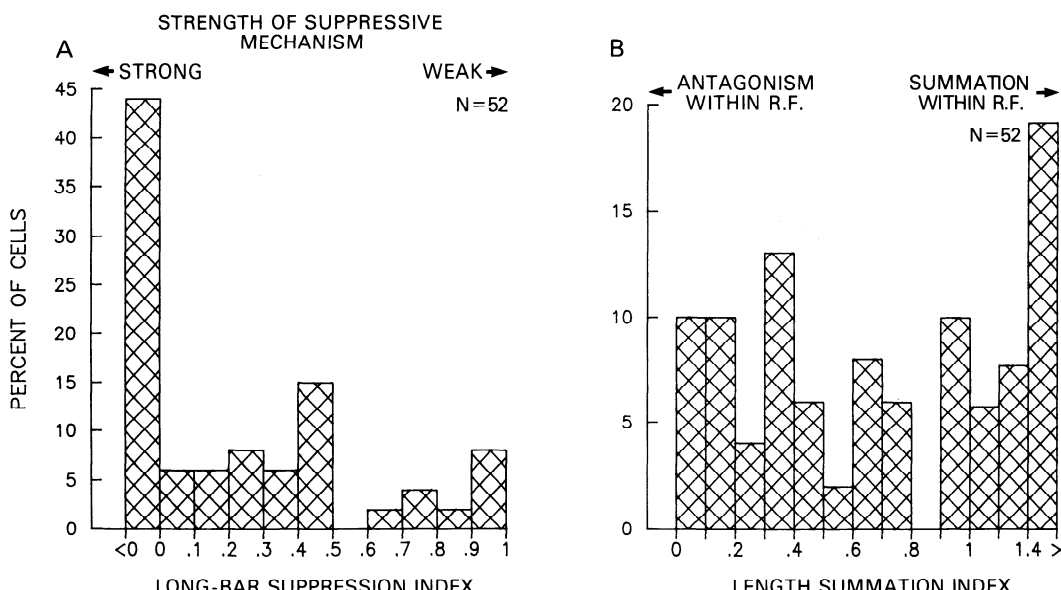


FIG. 8. Selectivity for bar length in V4. The distribution in A shows the suppressive effects of long bars. The abscissa plots the ratio between the response to the longest bar tested (typically 9°) and the response to the optimal bar for each cell. The distribution in B shows a comparison of the lengths of receptive fields of cells in V4 with the length of their optimal bars. The abscissa plots the ratio of the length of the optimal bar to the length of the receptive field.

fourths of these cells that responded to long bars had suppression originating from outside the receptive field only (e.g., Fig. 7, *B* and *D*), and the remainder were cells with no length suppression at all. Thus, a little over half the cells in V4 have both a length antagonistic mechanism located inside the field and a length suppressive mechanism located outside, a third have only a suppressive mechanism outside the field, and a tenth of the cells have no length antagonistic or suppressive mechanism at all.

As indicated in Fig. 8*B*, the optimal bar for a few cells was actually longer than the length of the receptive field. A small difference between the length of the optimal bar and the length of the field could easily be explained by small errors in plotting the receptive field or by the fact that receptive-field length sometimes fell between two tested bar lengths (e.g., see Fig. 7*D*). However, an examination of the length tuning curves of cells with indexes >1.5 suggested that many of those cells actually had silent summation zones beyond their mapped receptive fields.

**Width.** A total of 79 cells were tested quantitatively with bars varying in width from 0.05 to 6.4°. Seventy-one of these cells were tested with bars swept across the receptive field, and 40 cells were tested with bars flashed within the receptive field, including 32 cells that were tested with both. The range of optimal bar widths covered the full range of tested widths.

Width tuning curves to flashed and moving stimuli are shown in Fig. 7 for the same cells whose length tuning curves were described previously. Considering the tuning curves to flashed stimuli (solid curves) first, the four cells typify the same classes of response to stimulus width as they do to stimulus length. The cells illustrated in Fig. 7, *A* and *B* responded best to stimuli of 0.1 and 0.05° width, respectively, inside receptive fields that were at least 20 times wider. Neither cell responded at all to stimuli that extended the width of the receptive field, indicating that the field contained powerful antagonistic mechanisms along the width axis. By contrast, the cells illustrated in Fig. 7, *C* and *D* showed much greater summation to increases in stimulus width within the receptive field, responding best to stimuli that were 40 and 80% of the width of their receptive fields, respectively. The response of the cell in Fig. 7*C* was only slightly reduced (10% reduc-

tion in response) for a bar that filled the width of the field, and the response of the cell in Fig. 7*D* was not reduced at all. Both cells gave greatly reduced responses to stimuli wider than their receptive fields, indicating that powerful suppressive zones lie beyond the fields. As with stimulus length, the balance between summation and antagonism within the field, and the strength of suppression from beyond the field appeared to determine the particular shape of the width tuning curve to flashed stimuli for any given cell.

A difference between the length and width experiments arose in the response of cells to moving versus flashed bars. In the bar length experiments, length was varied along the dimension orthogonal to the direction of motion. Motion, therefore, did not affect the presence or absence of the two ends of the bar inside the field and should not have changed the shape of the length tuning curves. This was confirmed in 10 cells tested under both conditions. In the bar width experiments, however, motion could allow entry of the leading and trailing edges of a wide bar inside the field, edges that would have been outside the field in the flashed condition. Motion therefore should and did affect the shape of the width tuning curves for many cells.

As expected, the most substantial difference in response to moving versus flashed bars occurred to very wide bars. Many cells that responded poorly to wide bars when they were flashed responded well to the same bars when they were swept (velocity = 1–2°/s) across the receptive field. The cell illustrated in Fig. 7*D* is one such cell. Although the cell responded poorly to bars wider than 1.6° when they were flashed (solid curve), it showed no decrement in response to wide bars if they were moving (dashed curve). The response histograms of cells that responded to moving wide bars revealed that the response to the moving bar occurred when the leading or trailing edge of the bar passed over the receptive field. An example is shown in Fig. 9. The cell did not respond at all to a 6.4°-wide bar when it was flashed while centered on the receptive field, but responded well when it was moving. The response histogram for this wide moving bar (lower right in Fig. 9) shows two clearly defined peaks, one to the leading edge of the bar and one to the trailing edge. The activity between the peaks, when the receptive field was com-

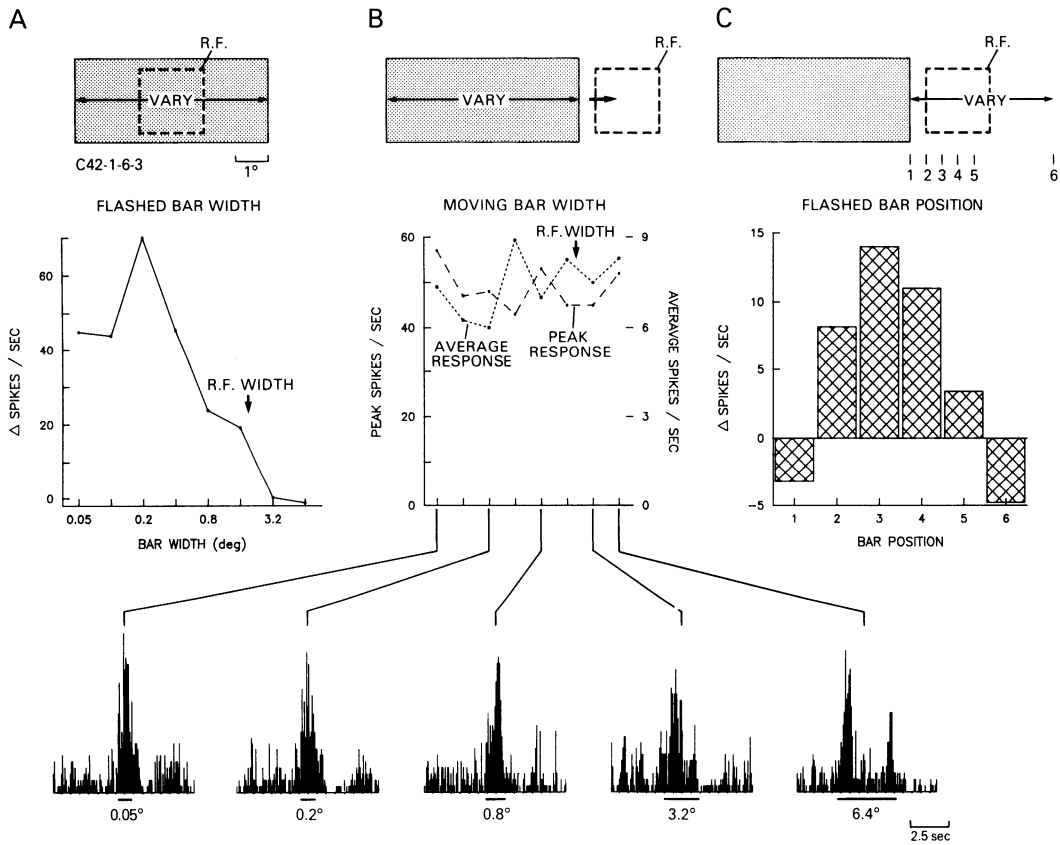


FIG. 9. Example of a V4 cell that exhibited selectivity for bar width when wide bars centered on the receptive field were flashed but not when the same bars were swept across the field. The width tuning curve in A is derived from the cell's average firing rate to white bars flashed within the receptive field for 1.28 s. The width tuning curves in B are derived from the cell's average (dotted curve) or peak (dashed curve) firing rate to bars swept across the field at 2°/s. The line under each histogram indicates the approximate time interval when at least one edge of the moving bar was inside the receptive field. The bar graph in C shows the average response to a wide (6°) bar flashed at several different locations.

pletely covered by the bar (and the edges located outside the field), was virtually at the base-line firing rate. For this cell, the width tuning curve was essentially flat regardless of whether the response was measured from the peak of the histogram (dashed curve) or from the average firing rate during the sweep of the bar (dotted curve). Some cells showed pronounced inhibition to wide bars during some portion of the sweep; as a result, the relative response of these cells to wide bars was larger if it was measured from the peak firing rate than if it was measured from the average firing rate.

The fact that a cell responds differently to moving and flashed wide bars can be understood in terms of our hypothesis regarding the

organization of the receptive field and its surround. With flashed bars, selectivity against wide bars results from activation of antagonistic mechanisms within the field or suppressive mechanisms beyond the field, or both. With moving bars, activation of these antagonistic or suppressive mechanisms will depend on the bar's position. For example, when the leading edge of the moving bar lies just inside the receptive field, there should be little activation of antagonistic mechanisms inside the field, and any suppression from the surround should be limited to one flank. A similar situation results when just the trailing edge of the moving bar lies just inside the field. By comparison, when a wide flashed bar is centered over the field, there should be maximal

antagonism from within the field, and suppression from the surround can arise from both flanks. Thus, the fact that a cell responds to a wide moving bar but not to the same bar flashed over the field may be due not to the motion per se, but rather to the fact that the moving bar will temporarily occupy receptive field locations that reduce any suppression or antagonism to wide bars.

It follows that a cell that responds to a moving but not a flashed wide bar covering the field should respond to the flashed bar if it is displaced, so that a single edge lies inside the field. This test was performed on six such cells, one of which was the cell described in Fig. 9. The cell was tested with a wide bar flashed at six different positions (see Fig. 9C). The cell did not respond at all (and appeared moderately inhibited) if the bar completely covered the receptive field (right edge at *position 6*, Fig. 9C) and even responded poorly if the bar covered most of the field (*position 5*). However, the cell gave a maximal response when the bar covered about a quarter of the receptive field width (*position 3*), consistent with the response elicited by the leading edge when the bar was moving. Similar results were obtained with the other five cells tested. Because the responses of such cells are so highly dependent on bar position, an individual cell of this type could not provide explicit information about bar width.

Although most V4 cells responded well to the edges of moving wide bars, this was not true of about a quarter of the cells. The cell illustrated in Fig. 10, for example (see also Fig. 7, A and B), responded poorly to wide bars regardless of whether they were moving or flashed. The response histograms of this and similar cells showed little response to the leading or trailing edge of moving wide bars, unlike the majority of cells in V4 (compare with Fig. 9). Poor responses to the leading or trailing edges of moving wide bars also distinguishes these V4 cells from cells in V1, which quantitative studies have shown almost invariably respond to the edges of moving bars (2, 58). Qualitative testing of this minority of V4 cells indicated that they did not respond well to flashed wide bars at any position, even when all but a small piece of the bar lay outside the receptive field, suggesting the presence of a particularly strong inhibitory flank.

To characterize the selectivity for bar width

quantitatively, we calculated for each cell two indexes that were analogous to the indexes used to characterize length selectivity. The first, the width suppression index, was calculated as follows

width suppression

$$= \text{response to widest bar/response to optimal bar}$$

This index reflects the strength of the mechanisms that reduce the response of a cell to wide bars. The value of the index would be 1.0 for cells that showed no reduction of response to the widest bar compared with the optimal and would be 0.0 for cells that did not respond at all to the widest bar. For flashed bars (Fig. 11A), the distribution of the index is highly skewed toward 0.0, indicating that most cells responded very poorly to wide bars centered on the receptive field. In fact, 25% of the cells had an index <0.0, indicating that a wide bar centered on the field actually reduced their activity below the base-line firing rate. When tested with moving bars (Fig. 11, B and C), about a quarter of the cells failed to respond well (indexes <0.3) to wide bars.

One difference between the distributions based on the average response to moving bars (Fig. 11C) and that based on the peak response (Fig. 11B) was that the former had a larger percentage of cells with an index of 0.0 or less, i.e., either inhibition or no response to wide bars. The primary reason for this difference appeared to be that some cells were inhibited during some portion of the sweep of the wide bar and excited during other portions. Because of the inhibition, the wide bar actually caused no net increase in average firing rate (and sometimes caused a net decrease) during its motion across the receptive field of these cells, although it did cause an increase in the peak response.

The second index used to quantify width selectivity was a width summation index, calculated as follows

width summation

$$= \text{width of optimal bar/width of the receptive field}$$

When measured with flashed bars, the magnitude of this index is determined both by how much width summation a cell exhibits within its receptive field and by the location of any width antagonistic mechanism. Low index values indicate a low degree of summation,

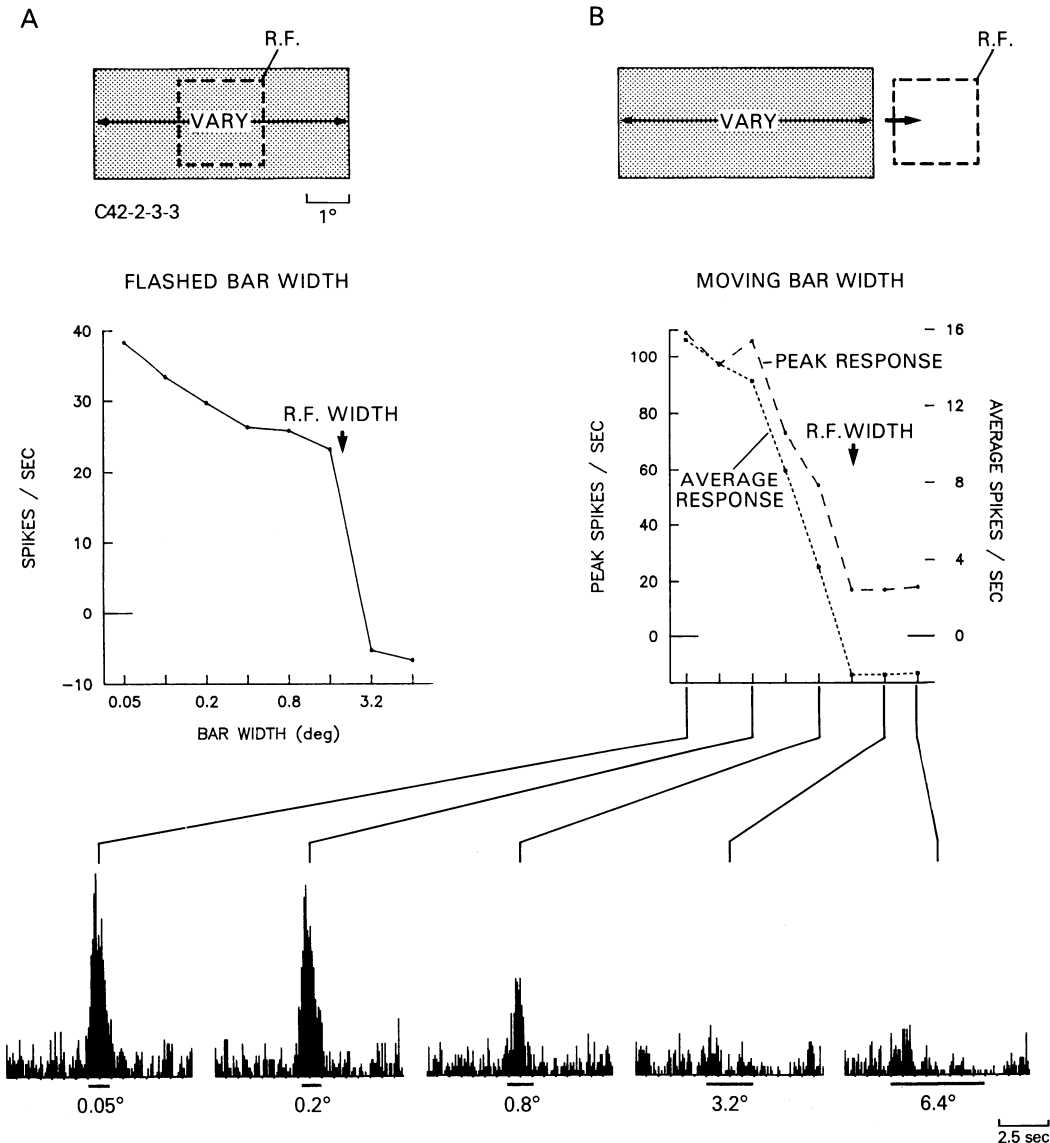


FIG. 10. Example of a V4 cell that exhibited selectivity for bar width both when bars were flashed within the receptive field and when bars were swept across the field. See legend to Fig. 9.

and, in particular, values much smaller than 1.0 suggest that width antagonistic mechanisms operate within the receptive field. High index values indicate a greater degree of width summation, with values near 1.0 or larger suggesting an absence of any width antagonistic mechanism inside the field (though not ruling out suppression from outside the field).

Fig. 11, D-F shows the distribution of the width summation index for both flashed and moving bars. With flashed bars (Fig. 11D),

there was a wide distribution of values, ranging from cells with an optimal bar <10% the width of the field (indexes <0.1) to cells with an optimal bar more than 150% the width of the field (indexes >1.5). Most cells showed evidence for at least some antagonistic mechanism within the receptive field (i.e., 90% had indexes <0.8). About half of these cells exhibited further reductions in response to bars wider than the receptive field, indicating the existence of an additional width suppressive

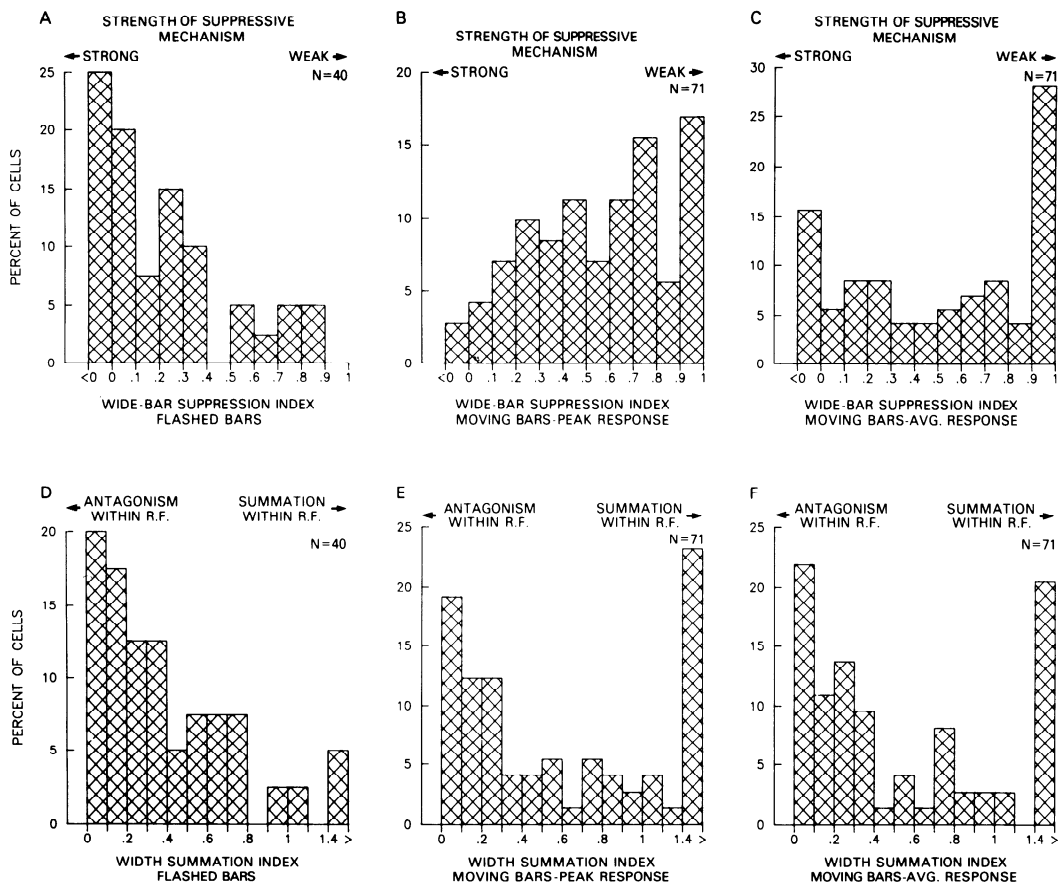


FIG. 11. The distributions in A-C show the suppressive effects of wide bars in V4. The abscissa of each graph plots the ratio between the response to the widest bar tested ( $6.4^\circ$ ) and the response to the optimal bar for each cell. The distribution in A is based on the response to flashed bars, that in B is based on the peak response to moving bars, and that in C is based on the average response to moving bars. The distributions in D-F compare the widths of receptive fields of cells in V4 with the width of their optimal bar. The abscissa of each graph plots the ratio between the width of the optimal bar and the width of the receptive field. The distribution in D is based on the response to flashed bars, that in E is based on the peak response to moving bars, and that in F on the average response to moving bars.

mechanism operating outside the field. The responses of the other half of the cells to bars the width of the field were too poor to allow determination of whether or not they were further reduced by increases in width beyond the field borders. Of the 10% of the cells with an index  $>0.8$ , all exhibited suppression originating from outside the receptive field. With moving bars, the distribution was similar to that obtained with flashed bars, but there were more cells for which the optimal bar was the widest bar tested, for reasons explained earlier.

**INTERACTION OF LENGTH AND WIDTH.** To gain a better understanding of how the length of a stimulus affected the width selectivity of

a cell and vice versa, we presented within the receptive fields of 12 cells a set of flashed bars with various combinations of length and width (centered on the receptive field). Within this two-dimensional response space, all but two cells showed a single peak of activity (see Fig. 12A), suggesting that the optimal length and width were relatively independent of one another. The location of the peak in the two-dimensional space varied from cell to cell, i.e., each cell preferred a bar with a different "shape", the same conclusion reached from the separate length and width tuning experiments described earlier (see Fig. 7). In this respect, cells in V4 of the macaque resemble those in area DL of the owl monkey (a possible

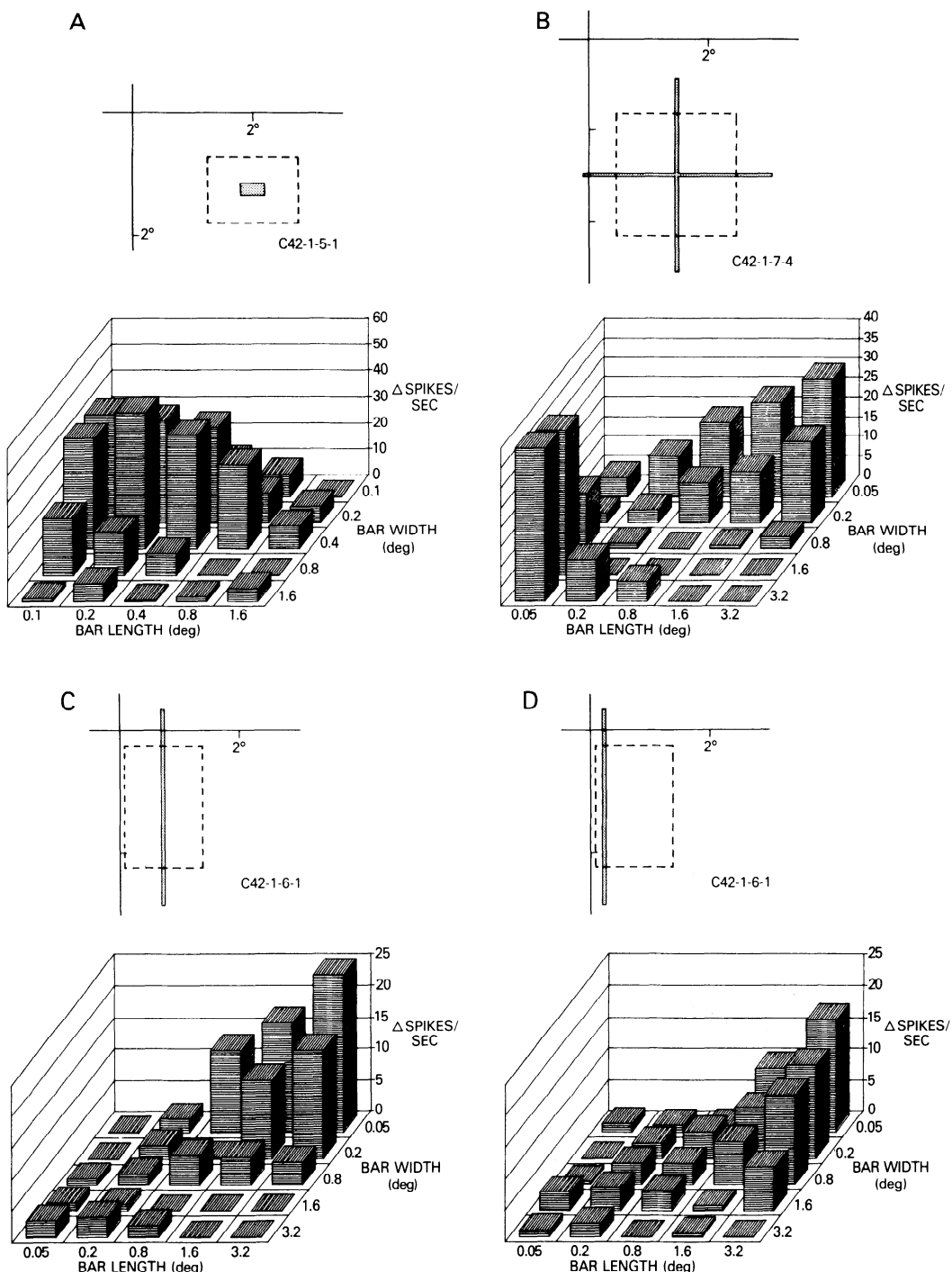


FIG. 12. Responses of 3 cells in V4 to bars of different lengths and widths. The responses of the 2 cells illustrated in *A* and *B* were measured to bars flashed at the center of the receptive field, whereas the responses of the third cell were measured to bars flashed both at the center of the field, *C*, and at the edge of the field, *D*. For each cell, the bars were on for 640 ms, and the drawing above each graph shows the receptive field and the size and location of the "optimal" bar. The cell illustrated in *B* responded best to bars either 3.2° long and 0.1° wide or 0.1° long and 3.2° wide, both of which are illustrated in the drawing. The bars used in *A* were blue, in *B*, black, and in *C* and *D*, green.

homologue of V4), which also show wide variations in the preferred shape of a bar inside the receptive field (49).

The two exceptional cells exhibited strong interactions between the optimal length and width. Each of the cells had two separate peaks at opposite corners in the response space, one peak to a bar with a vertical dimension of 0.1° and a horizontal dimension of 3.2° and the other peak to a bar with a vertical dimension of 3.2° and a horizontal dimension of 0.1° (Fig. 12B). That is, the shape of the optimal bar (long and thin) was constant over 90° changes in orientation. Neither cell showed orientation specificity when tested qualitatively. To our knowledge, such cells have not been described before in either striate or extrastriate cortex. The two cells responded as if they received converging inputs from width (narrow) and length (long) selective cells of all orientations, whose outputs were sent through a logical "OR" gate.

For 3 of the 12 cells, we repeated the presentation of the bars but this time centered the bars on a location near one edge of the receptive field rather than in the middle of the field. For two of these cells, shifting the bars to the edge of the field improved the response to wide bars and caused a shift in the peak of the response space. The third cell maintained its preference for a particular bar shape despite the change in position (Fig. 12, C and D), consistent with the properties of the minority of V4 cells described earlier.

#### *Experiments with gratings*

The experiments with bars revealed that V4 cells are highly sensitive to the spatial attributes of a stimulus. Furthermore, the relationship between the optimal size stimulus and the size of the receptive field suggested that two receptive-field variables might account for the spatial selectivity of a given cell: the balance between summation and antagonism within the excitatory receptive field, and the strength of the silent suppressive surround outside the excitatory field. In the experiments with gratings, our first goal was to determine whether the conclusions reached with bars could be extended to gratings, i.e., whether V4 cells were selective for the properties of gratings and whether their selectivity could be explained on the basis of the same two receptive-field mechanisms. In this context, gratings could

be regarded simply as complex patterns. Our second, and related, goal was to use gratings to explore the linear and nonlinear properties of cells in V4 and compare these properties with those reported for cells in V1.

**PEAK SENSITIVITY.** A total of 129 cells were tested with sine-wave gratings, and, of these, 112 responded well enough to yield tuning curves. The gratings varied in spatial frequency from 0.12 to 8 cpd in either full-octave increments (96 cells) or half-octave (16 cells). Typically, the gratings were drifted across the receptive field with an orientation and direction of motion that were optimal for the cell, and with a temporal frequency that was held constant at 1 cycle/s. Spatial frequency response curves were derived either from gratings that covered the complete face of the CRT screen ( $10 \times 10^\circ$  or  $10 \times 14^\circ$  in length and width) or from gratings that were (electronically) masked so that they did not extend beyond the borders of the receptive field in the length, the width, or either dimension (for a few cells that showed strong length antagonism inside the receptive field, the gratings were masked so as to be shorter than the field). The initial characterization of spatial frequency selectivity was based on the response curves derived from gratings restricted in length, or, for cells that were not tested with restricted gratings, on the response curves derived from gratings unrestricted in length and width.

All V4 cells responded to the drifting gratings with an elevation or depression of the mean firing rate, and some cells showed, in addition, some modulation of their response in time with the motion of the bars of the gratings across the field. Since the increase or decrease in mean rate was almost always larger than the modulated component of the response, we chose to use the mean rate in deriving the spatial frequency response curve for each cell.

The distribution of peaks in the spatial frequency response curves, shown in Fig. 13A, spans a range of six octaves, from 0.12 to 8 cycles per degree (cpd) (see examples in C of Figs. 14–16). Since this range spans the full range of spatial frequencies tested, the true distribution could even be somewhat wider than that indicated in Fig. 13. By comparison, the peaks of the spatial frequency response curves measured in foveal plus parafoveal V1

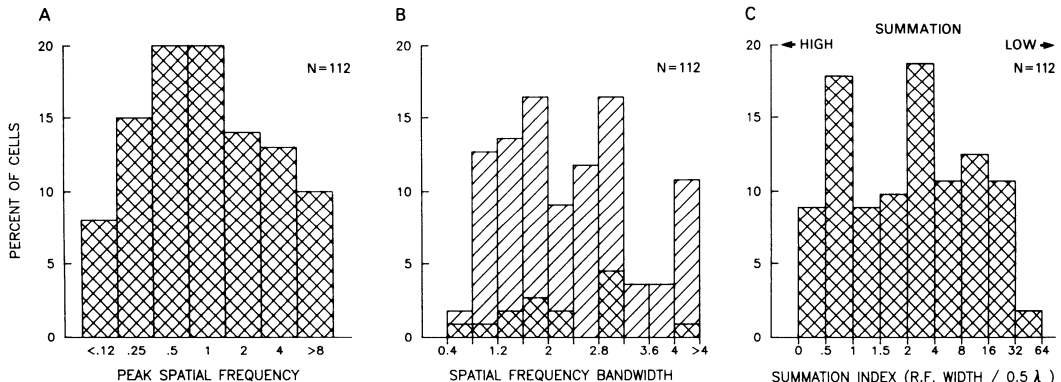


FIG. 13. Selectivity for gratings in V4. The distribution in *A* shows the optimal spatial frequencies (in cycles per degree) for 112 neurons. Cells were tested with gratings in full-octave increments, except for 16 cells tested at half-octave increments. Of the later group, cells whose best response occurred at a half-octave frequency value were placed in a full-octave bin based on the next-best response. The distribution in *B* shows the range of spatial frequency bandwidths in V4. Bandwidths contributed by cells tested with gratings in full-octave increments are shown with hatched bars, whereas bandwidths contributed by cells tested with gratings in half-octave increments are shown with cross-hatched bars. The distribution in *C* compares the width of the receptive field with the half-period of the optimal grating. Cells with high spatial summation within the receptive field have small values, and cells with low spatial summation have large values.

have been reported to range from 0.5 up to 16 cpd (16, 24) and in foveal plus parafoveal V2 from 0.25 up to 5.6 cpd (24). Thus, within the limits of the frequencies that we have tested, the distribution of peak spatial frequencies within the representation of 0–5° eccentricity in V4 is at least as wide as that within the corresponding representations of V1 and V2 and may even extend to lower frequencies than those reported in V1 and higher frequencies than those reported in V2. The difference between the highest peak spatial frequency found in V4, 8 cpd, and the highest found in V2, 5.6 cpd, could be accounted for in part by the fact that only 2 of the 11 V4 cells with peaks at 8 cpd were actually tested at 5.6 cpd (i.e., most cells were tested at 4 and 8 cpd). Consequently, some, but not all, of the cells with nominal peaks at 8 cpd might have actually had a peak response at 5.6 cpd.

In addition to spanning a wide range of optimal frequencies, V4 cells also spanned a wide range of tuning bandwidths. Bandwidths were calculated from the full width of the response curve at half-amplitude. For cells with peaks at or near the ends of the spatial frequency range tested, it was not always possible to calculate a full bandwidth, so for these cells we measured the half-bandwidth and then doubled it, though it is possible that cells with peaks at 0.12 cpd had low-pass rather than

band-pass spatial frequency tuning. The distribution of bandwidths is given in Fig. 13*B*. The most narrowly tuned cells had bandwidths of 0.5 octaves and the most broadly tuned cells had bandwidths >4.0 octaves, which means that the latter were not really “tuned” at all, having responded well to essentially all frequencies tested. The median bandwidth, 2.2 octaves, is considerably wider than the median bandwidth of 1.8 octaves reported by Foster et al. (24) for cells in parafoveal V1 and V2. The bandwidth difference between cells in V4 and cells in V1 and V2 is underscored by the fact that 43% of the cells in V4 had bandwidths >2.5 octaves compared with only 8% of the cells in V1 and 11% in V2 (24).

**SPATIAL FREQUENCY AND THE STRUCTURE OF V4 RECEPTIVE FIELDS.** The relationship between the optimal spatial frequency and the width of the receptive field varied widely from cell to cell. Some cells appeared to show a high degree of spatial summation to continuous regions of light (or dark) within the receptive field, responding best to gratings that covered the receptive field with a single “bar”. Other cells appeared to show more antagonism than summation to continuous regions of light or dark, responding best to gratings that filled the receptive field with many narrow bars.

To quantify the degree of summation within

the receptive field, we used a spatial summation index calculated as follows

$$\text{spatial summation} = \frac{\text{width of receptive field}}{\text{half-period of optimal grating}}$$

This index has been used to characterize spatial summation of cells in V1 of the cat (8, 46). The distribution of the index is shown in Fig. 13C. The index ranged from  $<1.0$ , meaning that less than a half-cycle of the optimal grating filled the receptive field, to 64, meaning that 32 cycles of the optimal grating were contained within the receptive field. Cells with small index values exhibited the highest degree of spatial summation within their receptive fields and cells with large index values exhibited the lowest degree of summation. Dean and Tolhurst (8) found that summation index values of between 1.4 and 1.9 could separate simple from complex cells in V1 of the cat. If we adopt a value of 1.7 to separate cells with high summation from cells with low summation in V4, then 36% of the cells in V4 behaved like simple cells, showing high summation (index  $<1.7$ ), whereas 64% of the cells in V4 behaved like complex cells, showing low summation (index  $>1.7$ ). For descriptive convenience, we will use this arbitrary criterion of 1.7 for distinguishing high from low summation cells in V4, without suggesting that they form two separate classes. Cells in V4 with high summation tended to prefer low spatial frequencies (mean = 0.48 cpd), whereas cells with low summation tended to prefer higher spatial frequencies (mean = 2.65 cpd).

For the few V4 cells tested with both gratings and bars, the summation measured with the two techniques appeared qualitatively similar. For the 14 cells with high summation to gratings (summation index  $<1.7$ ) that were tested with bars, the mean width of the optimal bar was 68% of the width of the receptive field. For the 17 cells with low summation to gratings that were tested with bars, the mean width of the optimal bar was only 12% of the width of the receptive field.

If a V4 cell summed linearly, it would in principle be possible to predict its receptive-field map derived with bars from the amplitude and phase of its spatial frequency response function and vice versa. Cells with a high degree of summation to gratings might be expected to show such a relationship,

whereas cells with a low degree of summation would not. Results from three cells on which we made such comparisons are illustrated in Figs. 14–16. For each cell we computed the line-spread function, or predicted receptive-field map, from the Fourier transform of the grating response curve. Although the phase of the cell's response to each frequency component was not available, the Fourier transform could be computed by assuming the receptive field was either even or odd symmetric (46).

The responses of a typical cell with a high degree of summation to gratings are illustrated in Fig. 14. The receptive field measured with light bars was  $1^\circ$  wide, and the half-period of the optimal grating was  $2^\circ$  (summation index = 0.5). From the Fourier transform of the grating response curve, the predicted width of the light bar response zone was  $1^\circ$ , which was identical to the measured width. The transform also predicted a broad shallow inhibitory zone in the surround, which we did not detect. Although the shapes of the measured and predicted excitatory fields were not identical, the correspondence in overall width was consistent with approximately linear summation, at least for light stimuli. Spatial summation to light increments was also evident from the cell's tuning curve for bar width, which showed a peak response to a light bar  $0.8^\circ$  in width. A nonlinear property of the cell, however, was evident from the cell's measured receptive-field map, which showed responses to both light and dark bars at some spatial locations. Since excitatory responses to both light increments and decrements at the same location violate the requirements for a linear system, they could not be predicted from the grating responses. Essentially all cells with high summation in V4 showed some degree of dark and light zone overlap and thus had a blend of linear and nonlinear properties. These cells could be described as being nearly linear for space but highly nonlinear for polarity of contrast. To the extent that simple cells in striate cortex exhibit complete separation of dark and light zones, then linearity for contrast polarity in V4 must be substantially degraded.

Unlike the V4 cells that exhibited high summation to gratings, there was a gross mismatch between the predicted and measured fields for V4 cells with low degrees of summation. The responses of two such cells are illustrated in Figs. 15 (summation index = 32)

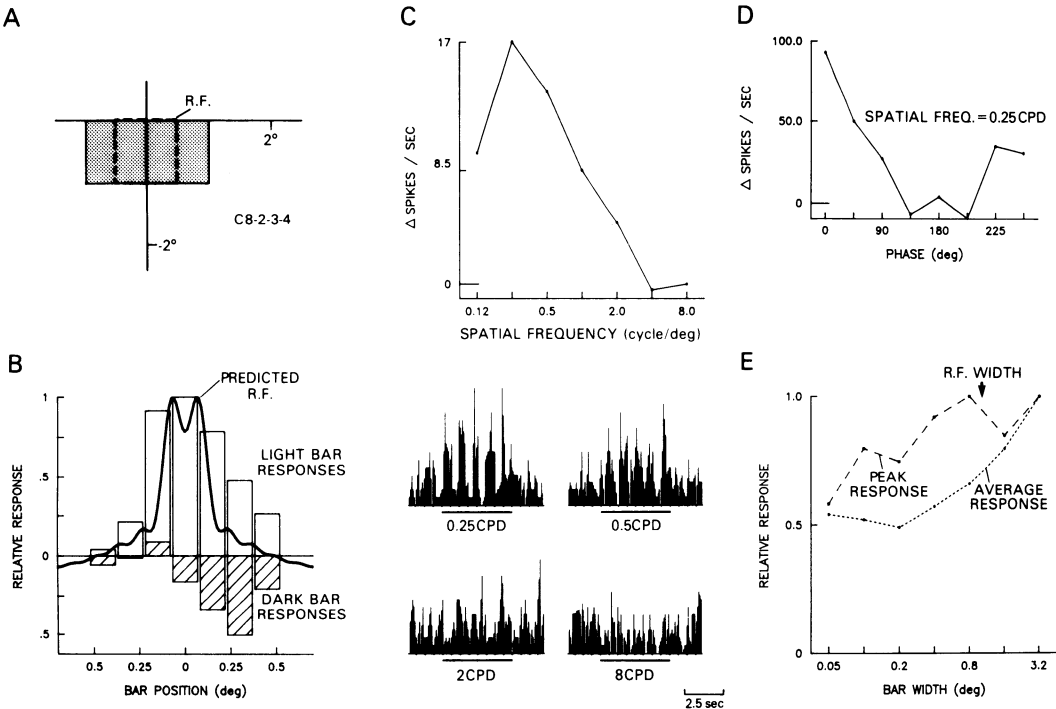


FIG. 14. Example of a cell with high spatial summation but whose receptive field contains overlapping dark and light zones. A drawing of the receptive field and a half-cycle of the optimal grating (grey) is shown in *A*. The measured light and dark zones of the field, along with the receptive field predicted from the Fourier transform of the grating response curve are shown in *B*. The amplitudes of the measured and predicted zones have been normalized to 1.0. Although the predicted receptive field has a broad, shallow dark zone extending for several degrees in both directions, for simplicity the full extent of this zone is not shown. The responses of the cell to drifting sine-wave gratings are shown in *C*. The ordinate of the graph is the average firing rate to gratings drifting at 1 cycle/s for 5 s on each of 10 trials. The histograms under the graph show the responses to gratings of 4 different frequencies. The bar under each histogram indicates the stimulation interval, during which 5 cycles of the grating passed over the receptive field. The response of the cell to a grating of optimal frequency (0.25 cpd) flashed for 640 ms per trial at several spatial phases is shown in *D*. The bar width tuning curve for moving white bars is shown in *E*.

and 16 (summation index = 5.6). The receptive field of the first of these cells consisted of overlapping dark and light zones, the most common field structure in V4, whereas the receptive field of the other cell consisted of a single (dark) zone, which was much less common. For the cell with overlapping zones (Fig. 15), the measured light bar response zone was  $2^\circ$  in width compared with a predicted width of  $0.1^\circ$ . This failure of spatial summation within the receptive field was also evident from the cell's tuning curve for bar width, which showed a maximal response to a  $0.1^\circ$  bar,  $\sim 7\%$  of the width of the receptive field. For the cell with a single dark response zone (Fig. 16), the measured and predicted zones were  $2$  and  $0.3^\circ$  in width, respectively. As with the first cell, the failure of spatial summation was

also evident from the tuning curve for bar width, which showed a maximal response to bars  $0.05^\circ$  in width,  $\sim 3\%$  of the width of the receptive field. Thus failures of spatial summation could occur regardless of whether the receptive field consisted of overlapping dark and light response zones or a single response zone.

**PHASE.** Sensitivity to the phase of gratings was tested in two ways. The first was by measurement of the waveform of a cell's response to drifting sinusoidal gratings. The responses of linear phase-sensitive cells should be highly modulated in time with the movement of the bars of the grating, as is true of the response of simple cells in V1 (e.g., see 15, 46) and is roughly true of the response of the V4 cell

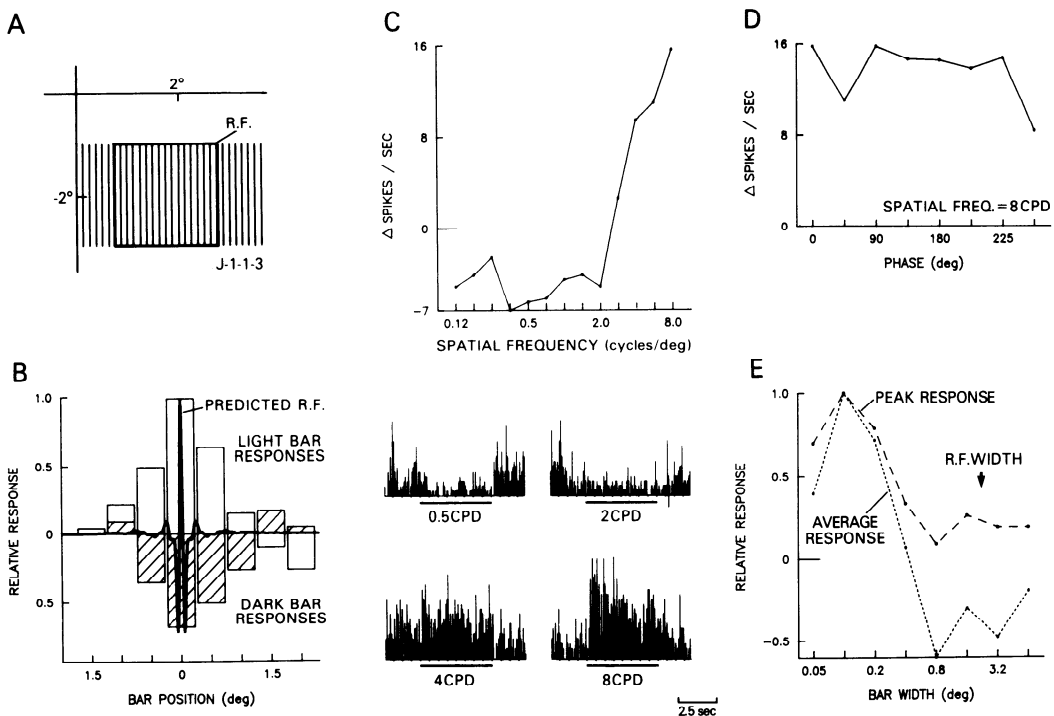


FIG. 15. Example of a cell with low spatial summation and whose receptive field contains overlapping dark and light zones. See legend to Fig. 14.

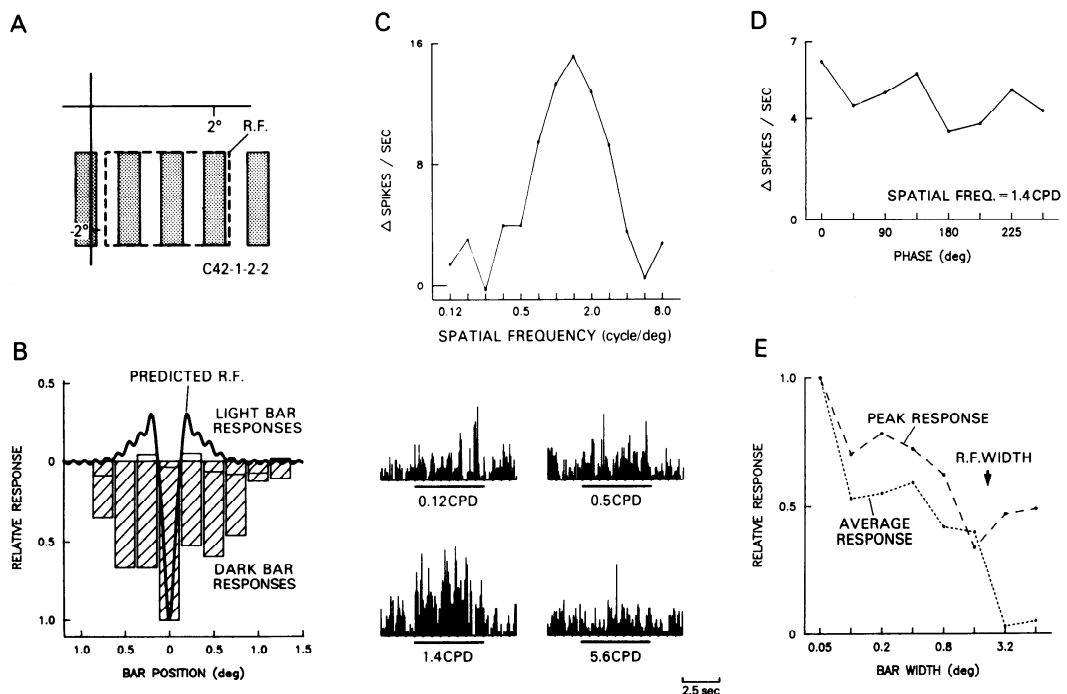


FIG. 16. Example of a cell with low spatial summation and whose receptive field consists of a single dark zone. The tuning curve for bar width was derived with black bars. See legend to Fig. 14.

shown in Fig. 14. The second was to measure the cell's response to flashed gratings presented at different spatial phases. The amplitude of response of linear phase-sensitive cells should be a sinusoidal function of grating phase, as is also true of simple cells in V1 (46, 63) and is nearly true of the V4 cell shown in Fig. 14.

As a measure of the relative modulation of response to drifting gratings, we computed the a.c./d.c. ratio (15). The a.c. response was defined as the amplitude of the fundamental frequency component (i.e. the component with the same temporal frequency as the grating) of the cell's response, and the d.c., as the mean firing rate. For both measures we subtracted out the average a.c. and d.c. components of the prestimulation activity. In order to select which grating responses to use for calculating the ratio, we added the a.c. and d.c. responses for gratings of all frequencies and chose the grating with the largest combined response. Because the d.c. component was normally much larger than the a.c., it contributed most to the combined response. In V1 of the monkey, simple cells are reported to have a.c./d.c. ratios  $>1.0$  (highly modulated), whereas complex cells are reported to have ratios  $<1.0$  (poorly modulated) (15).

The distribution of the a.c./d.c. ratio for both high summation cells (summation index  $<1.7$ ) and low (summation index  $>1.7$ ) is given in Fig. 17A. All of the cells with a.c./d.c. ratios  $>0.5$  (cross-hatched bars in the distribution) were cells that exhibited high summation to gratings, suggesting that cells with high summation are more sensitive to grating phase than cells with low summation, the same relationship found for simple versus complex cells in V1.

The tendency for cells with high summation to give more modulated responses to grating motion than cells with low summation can be predicted from their respective receptive-field properties. Cells with high summation respond best to gratings that fill the receptive field with a single broad bar. Any differential sensitivity of such a cell to light or dark should cause its response to modulate in time with the movement of broad light or dark bars across the field. The cell with high summation illustrated in Fig. 14 is one such cell. During the stimulation interval, five cycles of the optimal grating (0.25 cpd) passed over the receptive field, and, correspondingly, five clear peaks can be seen in the response histogram (Fig. 14C). By contrast, cells with low summation respond

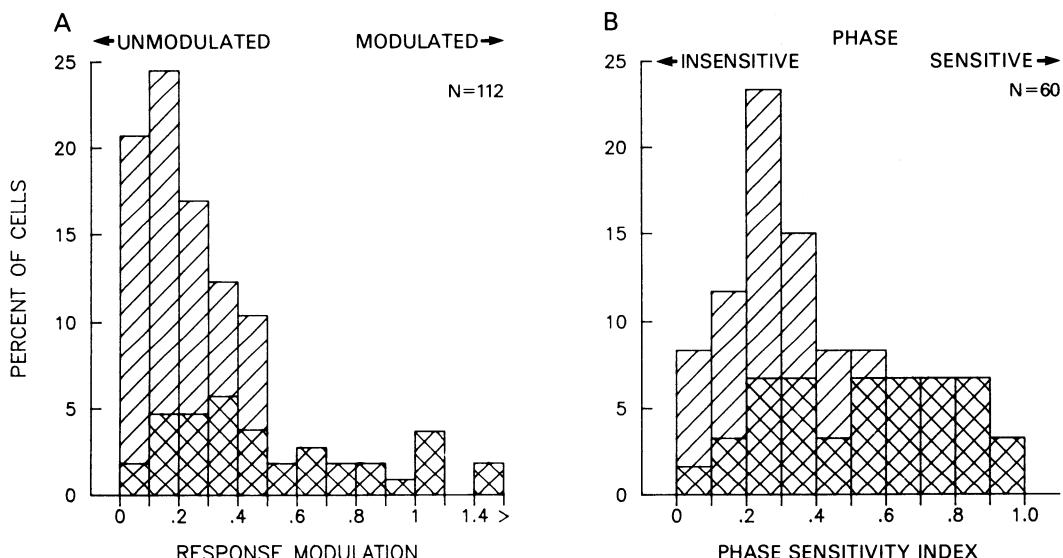


FIG. 17. Phase sensitivity in V4. The abscissa in A is the relative modulation (a.c./d.c. ratio) of a cell's response to drifting gratings of optimal frequency. The abscissa in B is the phase-sensitivity index for flashed gratings of optimal frequency. In both A and B, values contributed by cells with low summation are indicated with hatched bars, whereas those contributed by cells with high summation are indicated with cross-hatched bars.

best to gratings that fill the receptive field with many narrow bars. Even if such a cell were differentially sensitive to light or dark, movement of the grating would not affect the overall amount of light or dark in the field, and the cell's response should not be modulated. This behavior can be seen in the response histograms of the cells with low summation illustrated in Figs. 15 and 16.

Although cells with high summation showed greater modulation to drifting gratings than cells with low summation, even cells with high summation in V4 showed much less modulation to gratings on the average than has been reported for simple cells in V1. Although simple cells in V1 of the monkey have a.c./d.c. ratios  $>1.0$  (15), this was true of  $<16\%$  of the cells with high summation in V4. This relative loss of phase sensitivity in V4 is consistent with the results from receptive-field mapping. Although V1 simple cells respond to light and dark bars at spatially separate locations, nearly all cells in V4 respond to both light and dark bars throughout most or all of their receptive fields. Since the sinusoidal components of a light bar are identical in frequency but opposite in phase to those of a dark bar, the responsivity of V4 cells to light and dark bars is consistent with some loss of single-phase sensitivity.

A more direct measure of phase sensitivity was obtained from 60 cells in V4 tested with gratings of optimal frequency but variable phase flashed within the receptive field. Just as a linear cell should not respond to bars of opposite contrast at a single location, it should not respond to gratings of opposite phase. We therefore defined an index of phase linearity that was similar in form to the light-dark difference index used with bars. For each phase,  $i$ , ranging from 0 to  $179^\circ$ , the excitatory response was  $r(i)$ , a positive number, and the response to the opposite phase was  $r(i + 180)$ , a negative number. Phase linearity was then defined as

$$\text{phase linearity} = \frac{\sum |r(i) + r(i + 180)|}{\sum |r(i)| + \sum |r(i + 180)|}$$

The index ranges from 0.0, when two gratings that are  $180^\circ$  opposite in phase always elicit the same response, to 1.0, when two gratings  $180^\circ$  opposite in phase never both elicit responses. A classic simple cell in V1 would have

an index of 1.0 and a classic complex cell would have an index of 0.0.

The distribution of the phase linearity index both for cells with high summation and for cells with low summation is given in Fig. 17B. The distribution shows that nearly all V4 cells gave some response to gratings of opposite phase (indexes  $<1.0$ ). This is consistent with the response they gave to bars of opposite contrast. Yet, many V4 cells were not indifferent to phase. For example, a third of the cells showed more than a 3:1 response ratio to gratings of opposite phase (indexes more than 0.5). As expected, virtually all of these cells that exhibited some phase sensitivity to flashed gratings showed high summation (cross-hatched bars in Fig. 17B) and gave modulated responses to drifting gratings (see Fig. 14). Cells with low summation (single-hatched bars in Fig. 17B) tended not to exhibit phase sensitivity under either condition (see Figs. 15 and 16).

**GRATING SIZE.** A total of 36 cells were studied with at least two out of three sets of gratings that differed in overall size. The first set of gratings was "unlimited" in length and width, i.e., extended to the limits of the  $10 \times 10^\circ$  or  $10 \times 14^\circ$  CRT screen; the second set was unlimited in width but was limited in length to that of the excitatory receptive field; and the third set was limited in both length and width to the dimensions of the receptive field.

For most V4 cells, the closer the overall size of the gratings was to the dimensions of the receptive field, the larger was the response (see Fig. 18). Of 17 cells tested with full size gratings versus gratings restricted in length, 13 gave larger responses to the smaller gratings, and the average response was 2.4 times the response to the larger. Of nine cells tested with gratings restricted only in length versus gratings restricted in both length and width, seven gave larger responses to the smaller gratings, and the average response was 1.7 times the response to the larger. Finally, of 20 cells tested with full-size gratings versus gratings restricted in length and width, 15 gave larger responses to the smaller gratings, and the average response was 2.1 times the response to the larger. These findings were obtained from both high- and low-summation cells. Along with the results from the length and width tuning experiments, the results provide further evidence

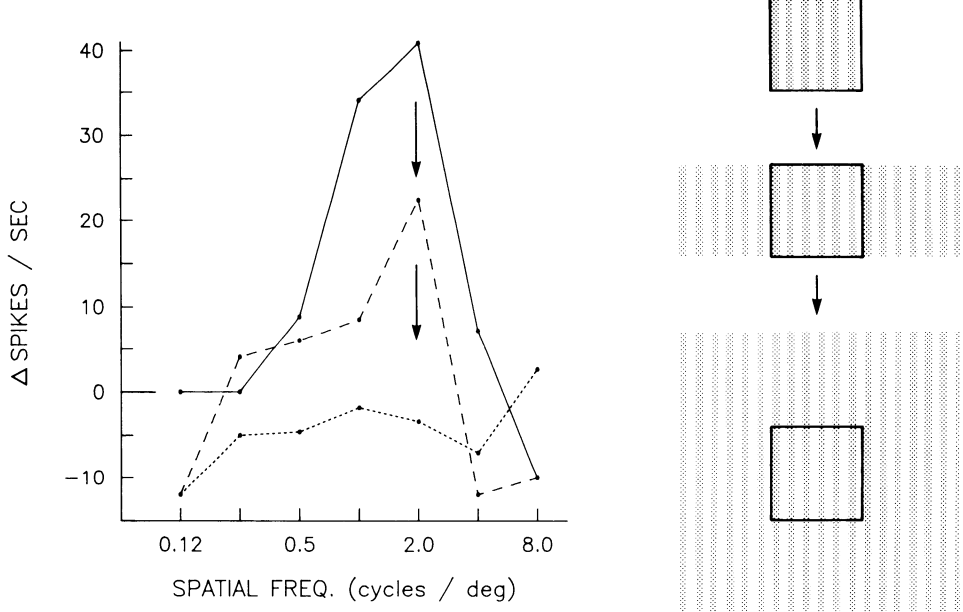


FIG. 18. A comparison of the spatial frequency response curves of a V4 cell tested with gratings restricted to the excitatory receptive field (solid curve), with gratings restricted to the length of the receptive field but unrestricted in width (dashed curve), and with gratings unrestricted in length or width (dotted curve).

for silent suppressive mechanisms beyond the classic receptive field. In fact, for nearly all the cells tested with both bars and gratings, the evidence for suppression along the length or width axis was consistent across stimuli. Preliminary results indicate that the suppressive effects of a stimulus outside the receptive field is often maximal if it matches the spatial frequency, phase, and orientation of the stimulus inside the field (see 14).

Since we did not systematically compare responses with gratings shorter and longer than the receptive field, we could not test specifically for the antagonistic interactions along the length axis inside the field that had been revealed during the experiments with bars. However, at least a third of the cells that exhibited low summation to gratings had little or no orientation specificity. These cells responded best to gratings that covered the receptive field with many narrow bars regardless of orientation, and, hence, appeared to exhibit antagonistic interactions along every axis inside the receptive field.

**SQUARE-WAVE GRATINGS.** In the course of the experiments with drifting sine-wave grat-

ings, we noted that a few cells (17/129) responded poorly or not at all to gratings but nonetheless gave good responses to individual bars swept across the field (the results from these cells were not included in the indexes of spatial frequency selectivity). In an attempt to understand the reason for this difference, we tested nine of the cells with drifting square-wave gratings, which had sharp edges like the bars, but were repetitive patterns like the sine-wave gratings. Although the luminance and contrast of the square-wave and sine-wave gratings were identical, all of the cells responded much better (600% mean improvement in response at the peak of the tuning curve) to the square-wave than to the sine-wave gratings, suggesting that edge sharpness was the critical variable. Responses from one such cell are illustrated in Fig. 19. Since we only tested square-wave gratings on cells that gave little or no response to sine-wave gratings, we do not know how prevalent the preference for square-wave gratings or sharp edges is in V4. The results from the nine cells tested, however, suggest that edges might be explicitly represented in V4, unlike the case in V1 (2, 58).

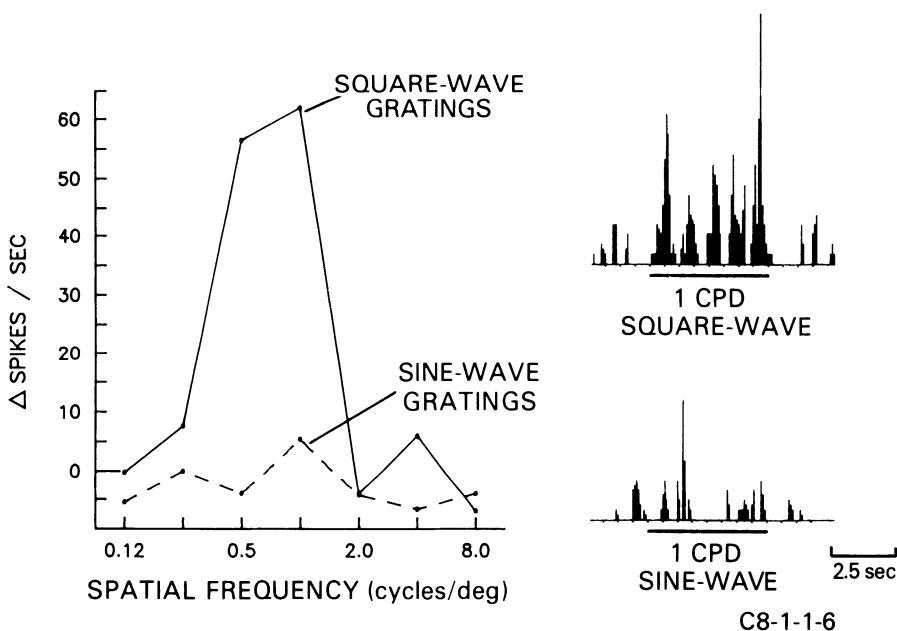


FIG. 19. A comparison of the spatial frequency response curves of a V4 cell tested with sine-wave gratings and square-wave gratings. The receptive field of the cell was  $0.7^\circ$  wide by  $0.6^\circ$  tall. The histograms on the right show the responses to the optimal sine-wave and square-wave gratings. The bar under each histogram indicates the stimulation interval, during which 5 cycles of the grating passed over the receptive field.

## DISCUSSION

### *V4 is both a "color area" and a "form area"*

The spectral properties of V4 cells were examined extensively by Zeki (74–76, 78, 79), who, in a series of studies, reported that V4 contained a very high proportion of wavelength-selective cells, that many V4 cells failed to respond to white light, that some V4 cells were more narrowly tuned to wavelength than were any cells in V1, and that some V4 cells appeared to exhibit color constancy. These results, in conjunction with Zeki's findings that V2, V3, V3A, and MT contained far fewer, if any, wavelength selective cells (73, 77), led Zeki to propose that V4 was a cortical area specialized for the analysis of color. Other studies of the spectral properties of cells in V4, however, did not support all of Zeki's conclusions. These studies reported that only a small proportion of cells in V4 were highly selective for wavelength, that this proportion was no greater than that found in V2, and that the most selective cells in V4 were no more narrowly tuned for wavelength than cells in either V1 or V2 (9, 23, 37, 55). Most recently, we have found that the large majority of cells in

V4 are indeed tuned to wavelength, supporting Zeki, but many are rather broadly tuned and most respond to white light (54). Yet, in spite of the absence of very narrow tuning, we found that most V4 cells show spectral interactions between their excitatory receptive fields and large suppressive surrounds. This result, in conjunction with Zeki's (76, 78, 79) findings that many V4 cells exhibit color constancy, suggests that color is, in fact, an important stimulus attribute in V4.

In addition to the selectivity of V4 cells for wavelength, the results of the present study demonstrate for the first time that the large majority of cells are also selective for stimulus form. The responses of many V4 cells are selective for the orientation, length, and width of bars and the spatial frequency, phase, and size of sinusoidal gratings. Thus V4 appears to be as much a form area as it is a color area. This interpretation is also supported by the results of a recent behavioral study by Heywood and Cowey (unpublished data), who found that animals with lesions of V4 are severely impaired in orientation and pattern discrimination as well as in wavelength discrimination.

The presence of both form- and color-selective cells in V4 is consistent with the known anatomical connections of this area. V4 receives its visual inputs from striate cortex primarily by way of area V2 but also receives inputs from V3 (67, 68, 73). The zones in V2 that project to V4, namely the thin cytochrome oxidase stripes and the interstripe regions, contain cells selective for wavelength, orientation, size, and binocular disparity (18, 32, 62), and area V3 contains cells selective for direction of motion (7). Thus V4 is a site of convergence for many types of visual information. Likewise, V4 provides the primary inputs to inferior temporal cortex (11, 67), which also contains cells selective for many different stimulus features, including color, shape, and texture (10, 30).

The fact that V4 contains cells selective for many different features, including both color and form, argues against the notion that each of the prestriate visual areas processes a different stimulus attribute in parallel with one another. Rather, information appears to flow through the visual cortex along just a few major pathways (14, 66, 69). One pathway is directed from the occipital lobe into the temporal lobe and is crucial for visual recognition of objects. This pathway, involving primarily portions of V1, V2, and V4 as well as the inferior temporal cortex, is organized as a serial hierarchy in which many object features, such as shape, color, and orientation, are processed within each of the areas along the route. A second pathway is directed from the occipital lobe into the parietal lobe and plays an important role in the ability to judge spatial relationships among objects and in visuomotor performance. Although not all of the cortical components of this pathway and their neuronal properties are established, area MT, medial superior temporal (MST) area, ventral intraparietal (VIP) area, and area 7a, along with portions of V1, V2, V3, and V4 appear to play a major role in it, and motion selectivity appears to be one of the prevalent neuronal properties (66).

Although the visual areas along the pathway from V1 into the temporal lobe appear to process both form and color, recent evidence suggests that there might be a partial segregation of form and color processing within individual areas. In V1, it has been reported that the cytochrome oxidase blobs of layers 2 and 3 contain primarily unoriented cells, most of which

(75%) are "wavelength selective", whereas the nonblob portions of these layers contain primarily oriented cells, most of which (61% in the foveal representation) are not wavelength selective (39; but see 43, 71). Likewise, in V2, it has been reported that the thick cytochrome oxidase stripes contain primarily oriented and directional cells without wavelength selectivity, that the thin cytochrome oxidase stripes contain primarily unoriented cells selective for stimulus size (32) and wavelength (18, 32, 62) and the interstripe regions contain cells variously reported to be selective for wavelength but not orientation (18) or orientation but not wavelength (32, 62). In V4, Zeki (77) has reported variations in the proportions of wavelength selective cells on neighboring penetrations, and, in addition, reports wavelength-selective cells to be concentrated within the lunate and superior temporal sulci and non-wavelength-selective cells to be concentrated on the gyrus. We have found both a high proportion of cells selective for wavelength and a high proportion of cells selective for form on the prelunate gyrus, but cannot yet say whether the cells most highly selective for wavelength and the cells most highly selective for form are anatomically separate. However, since the vast majority of cells in V4 show some selectivity for wavelength (54), and the vast majority also show some selectivity for form, there must be considerable overlap of color and form processing.

#### *Comparison with striate cortex*

So far, all stimulus qualities represented by cells in V1 appear to be represented by cells in V4 as well. Many cells in both areas are sensitive to stimulus orientation, length, width, spatial frequency, phase, contrast, or combinations of these properties, and a few cells in both areas are also sensitive to direction of motion. Significantly, even though receptive fields in V4 are much larger than in V1, the ability of cells in V4 to distinguish very fine features may also be comparable with that of cells in V1. The cells most narrowly tuned for orientation in V4 have bandwidths of <30°, which is only slightly broader than the most narrowly tuned cells in V1 (16, 57). In terms of cell "acuity", we found that some cells in V4 gave a peak response to gratings of the highest frequency tested, 8 cpd. It is possible that the responses of some of these cells would

have peaked at 16 cpd, the highest frequency found in V1 for a small number of cells (15, 24). Moreover, some cells in V4 give a peak response to bars 0.05° in width (or possibly narrower), which is about the receptive-field width of many cells in the foveal representation of V1 (56). These correspondences between V4 and V1 cells in their sensitivity to stimulus form parallel the results of other studies showing that the spectral bandwidths of cells in V4 are comparable with those of cells in V1 (9).

The receptive-field properties of cells in V4 suggest a number of ways in which individual cells in V4 may code form even more explicitly than individual cells in V1. First, many cells in V4 respond maximally to a stimulus of a particular length and width within a large receptive field, and the selectivity of some cells for a particular shape is maintained over shifts in stimulus position. In this respect, cells in V4 are similar to those of cells in area DL of the owl monkey (a possible homologue of V4), which are also selective for bars of particular length and width inside a large receptive field (49). There may also be a similarity between cells in V4 and the "spot" (5) or "complex unoriented" (32) cells described in V2, but it is not yet clear if the V2 cells are indeed tuned to spots or to certain combinations of length and width, as are the cells in V4. In any case, no cells in V1 of the monkey have been reported to have properties such as those in V4. Furthermore, while some cells in V1 are tuned to stimuli the length of the receptive field, quantitative experiments with moving bars have shown that hardly any cells are tuned to stimulus width (2, 58). The generalization of response over spatial location found in V4, which is continued even more dramatically in the inferior temporal cortex (10, 30, 59), may contribute to the perceptual equivalence of objects over retinal translation (29, 60). Although the price of this operation might seem to be a loss of spatial localization, it has been shown in awake behaving monkeys that when a monkey attends to a location within the receptive field of either a V4 or inferior temporal cell, the cell responds as if the receptive field had contracted around the attended location, i.e., the responses to stimuli at other locations within the field are greatly attenuated (44). Thus spatial localization of specific features may be maintained within the locus of visual attention.

A second way individual cells in V4 may code form more explicitly than individual cells in V1 is also related to receptive-field size. Because of their larger receptive fields, cells in V4 can not only generalize their response over a larger retinal area, but can code larger stimulus features than individual cells in V1. Some cells within the representation of the central 5° in V4, for example, respond optimally to bars up to 2–3° or more in length and width inside their receptive fields and less well to bars that are either larger or smaller. Such bars are far larger than receptive fields in foveal or parafoveal V1. Although V1 cells will, of course, respond to the edges of large stimuli, an individual V1 cell stimulated by the edge of a bar probably cannot distinguish between an edge that belongs to a bar 2–3° in width and an edge that belongs to a bar that is much wider. Likewise, some cells in V4 show band-pass spatial frequency tuning to much lower spatial frequencies (i.e., gratings with wider bars) than any cells in V1 (16, 24).

A third, and possibly the most important, receptive-field difference between cells in V4 and V1 is the large silent suppressive zones surrounding the excitatory receptive fields of cells in V4. We term these suppressive zones silent since stimulation of the zones does not normally inhibit a cell's spontaneous activity but can have a powerful effect on the response of a cell to a receptive-field stimulus. Because of these suppressive zones, many cells respond poorly to bars or gratings that extend beyond the receptive field in any direction. Preliminary results from varying the receptive field and surround stimuli independently indicate that the stimulus-selective properties of the excitatory receptive field and the suppressive surround are often matched, i.e., the orientation or spatial frequency of the surround stimulus that elicits maximal suppression is the same that elicits maximal excitation inside the receptive field (14). Likewise, we have found that the wavelength of the surround stimulus that elicits maximal suppression is the same as that which elicits maximal excitation inside the receptive field (14, 54). As a consequence, many V4 cells respond maximally to a stimulus only if it stands out from its background on the basis of a difference in form or color.

Although there are suppressive zones beyond the excitatory receptive fields of some cells in V1, especially along the length axis

(35, 56), the selectivity of these surrounds for form and color is not yet well established in the monkey. Furthermore, we suspect that suppressive surrounds in V1 are considerably smaller than those in V4. Surrounds of receptive fields in V4 can range up to 30° or more in diameter and extend up to 15° across the vertical meridian into the ipsilateral visual field (45). Although the total size of suppressive surrounds of cells in V1 of the monkey have not been measured, we do know that the surrounds of fields that lie on the representation of the vertical meridian in V1 do not cross more than 1° into the ipsilateral visual field (unpublished data).

What is the significance of the large size of the suppressive surrounds in V4? Local interactions between receptive fields and their surrounds, such as those that take place in the retina, lateral geniculate nucleus, and V1 (3, 42) presumably serve to enhance contrast at borders. Given the large scale of the interactions in V4, we wonder if this organization might serve more global perceptual mechanisms. In the spectral domain, the surrounds may contribute to the mechanism for color constancy, which is crucial for accurate color identification (14, 54). Indeed, Zeki (79) has reported that some V4 cells exhibit color constancy, whereas cells in V1 do not. In the spatial domain, we have speculated that the surrounds contribute to the selectivity of some V4 cells for stimulus shape and also help maintain the selectivity of some cells for a particular shape over changes in stimulus location. Finally, in both domains, the sensitivity of V4 cells to form or color differences between a stimulus and its background may be useful for figure or ground separation, or "breaking camouflage", an essential element of both form and color vision. A similar role for extrastriate cortex has been suggested by Allman et al. (4) based on the responses of extrastriate neurons to differential motion between the receptive field and its surround. In area MT of the owl monkey, for example, the response of a cell to a particular direction of motion within the excitatory receptive field is suppressed by the same direction of motion in a large, otherwise silent, surrounding region whose size may approach that of the entire visual field (4). Whether specific types of receptive field-surround interactions are confined to particular visual areas or, as recent evidence suggests

(6, 17, 24, 53, 72), are present in all visual areas, remains to be determined.

SIMPLE AND COMPLEX CELLS. In their classic 1962 paper on the properties of cells in striate cortex of the cat, Hubel and Wiesel (33) described two classes of cells that they termed simple and complex. The receptive-field properties of simple cells were summarized on page 110 as follows:

"(1) they [receptive fields] were subdivided into distinct excitatory and inhibitory regions; (2) there was summation within the separate excitatory and inhibitory parts; (3) there was antagonism between excitatory and inhibitory regions; and (4) it was possible to predict responses to stationary or moving spots of various shapes from a map of the excitatory and inhibitory areas."

It was subsequently recognized that these simple-cell receptive-field properties were precisely the properties one would expect of a linear system, whereas the absence of any of these properties would be characteristic of a nonlinear system, or a complex cell in the Hubel and Wiesel terminology (see 61). From the experimenter's point of view, the advantage of a linear system is that knowledge of the system's response to a very small set of stimuli, such as sine-wave gratings of different frequencies and orientations or points of light at different spatial locations, allows one to predict the system's response to the much larger set of stimuli that can be produced by the addition of stimuli from the original small set. Because it is possible to completely characterize the behavior of such a system, linearity has become practically the null hypothesis of visual neurophysiology.

Since the original findings of Hubel and Wiesel, both linear and nonlinear, or simple and complex, cells have been described in V1 and V2 of the cat and monkey (28, 34, 38, 40, 46, 47, 50, 52, 56, 63, 64). In V4, we found that nearly all receptive fields have overlapping light and dark zones, and, on that basis alone, V4 cells are nonlinear and resemble complex cells. Indeed, since most V4 cells have silent suppressive zones located beyond their excitatory receptive fields (an additional type of nonlinearity), they would probably be placed in the "hypercomplex" class in the original

Hubel and Wiesel scheme. Yet, in certain other respects, the properties of V4 cells appear to span a continuum, with cells at one end most resembling simple cells and cells at the other end most resembling complex cells.

At the "simple" end of the V4 continuum are the cells that exhibit "high summation". These cells appear to show nearly linear (or at least monotonically increasing) spatial summation to bars or gratings within their excitatory receptive fields, as do simple cells in V1. Furthermore, high-summation cells with a strong preference for light or dark stimuli within their excitatory receptive field may show nearly the same degree of phase sensitivity as simple cells. In fact, the near linearity of the high-summation cells for space but not contrast polarity suggests that they might receive inputs from two types of linear mechanisms, a light excitatory (dark inhibitory) one and a dark excitatory (light inhibitory) one, which are simply "OR" gated to give V4 cells their mixed light and dark responses (see 64). These linear input mechanisms might be simple-like cells in V2 (24) that are tuned to low frequencies and dominated by either light or dark responses. If this reasoning is correct, then it might be possible to predict the response of such a V4 cell to an arbitrary stimulus (confined to the excitatory field) by calculating the products of the stimulus intensity profile and the light and dark portions of the receptive-field map separately, and then taking one of the two results. Contrast polarity itself might be extracted by comparing the responses of cells differentially sensitive to light with the responses of cells differentially sensitive to dark. We have not yet tested these possibilities.

At the "complex" end of the V4 continuum are the cells that exhibit low summation. Like the cells that exhibit high summation, these cells also respond to both light and dark bars inside their excitatory fields, often with a strong preference for one or the other. Unlike the high summation cells, however, they respond best to a bar that is much narrower than the excitatory field and to gratings that cover the excitatory field with many narrow bars. Thus, these cells show primarily antagonism within their receptive fields rather than summation, and there is no obvious way to predict their response to an arbitrary stimulus from their receptive-field map alone. It is possible that these cells sum the outputs of many com-

plex cells in V2 to achieve their larger receptive fields. If some of the V4 cells summed the outputs of end-stopped complex cells (i.e., hypercomplex cells), this might explain the properties of cells that exhibited low summation to both length and width, i.e., selectivity for a short narrow stimulus within a large receptive field.

It is important to emphasize that the high-to-low-summation axis in V4 is really a continuum, and that cells do not naturally fall into two classes. Whereas Hubel and Wiesel (33) reported that cells in V1 of the cat fell naturally into either the simple or complex cell classes, more recent results suggest that a continuum of properties may exist in V1 as well. Spitzer and Hochstein (63, 64), for example, have reported that many complex cells in V1 of the cat have mixed linear and non-linear properties, and Dean and Tolhurst (8) have recently reported that indexes of receptive-field discreteness, spatial summation, and modulation to drifting gratings are continuously distributed in V1, much as we found in V4.

What is the functional significance of a simple to complex distinction that begins in V1 and is maintained in some form at least through V4? In V1 of the monkey, complex cells have a somewhat higher peak spatial-frequency range (15), encompass more cycles of an optimal grating within their receptive field (24), and are far more likely to respond to dynamic random dot stereograms than simple cells (51). Furthermore, in V1 of the cat, Hammond and Mackay (31) have reported that only complex cells respond to the motion of visual noise fields. All of these results suggest that complex cells may be particularly suited for the analysis of textures (31). Indeed, Zucker (80) has proposed a computational model of texture discrimination based on the properties of complex cells. In Zucker's model, complex cells play an important role in extracting the global orientation or "flow" of texture fields and signaling texture discontinuities, whereas simple cells are more useful for the analysis of solid contours.

An analogous distinction may be carried through in V4, where low-summation cells respond to higher spatial frequencies than high-summation cells and respond better to gratings that cover the receptive field with many cycles. It may be an oversimplification, however, to

speak only of textures versus contours. Visual features can occur over a wide range of sizes, shapes, and densities, and it may be that the wide variations in spatial summation found among V4 receptive fields simply reflects the need to code, or spatially "filter", such a wide range of features. Thus the cells with the highest degree of summation within their receptive fields may provide information about the largest stimulus features, whereas the cells with the lowest summation may provide information about the smallest or most finely spaced features (including textures, as an extreme case). Moreover, because summation along the width axis appears to occur independently of summation along the length axis, a cell that exhibits spatial summation for length but antagonism for width could provide the most information about long thin features, whereas a cell that exhibits antagonism for both length

and width could provide the most information about short thin features.

#### ACKNOWLEDGMENTS

We thank Mortimer Mishkin for his support in all phases of the experiment. Francisco de Monasterio and Jeffrey Moran made many useful suggestions during the course of the work, and Mortimer Mishkin, Leslie Ungerleider, Hedva Spitzer, and Daniel Pollen read early drafts of the manuscript. We are especially grateful to Jeffrey Moran for help in programming and to Bonnie McCrane for processing the histological material.

S. J. Schein was supported in part by Research to Prevent Blindness, Inc. and the Massachusetts Lions Research Fund.

A preliminary account of this work was presented at the 1983 meeting of the Society for Neuroscience (13).

Address reprint requests to: R. Desimone, Laboratory of Neuropsychology, National Institute of Mental Health, Building 9, Room 1N107, Bethesda, MD 20892.

Received 23 May 1986; accepted in final form 30 October 1986.

#### REFERENCES

- ALBRIGHT, T. D. Direction and orientation selectivity of neurons in visual area MT of the macaque. *J. Neurophysiol.* 52: 1106-1130, 1984.
- ALBRECHT, D. G., DE VALOIS, R. L., AND THORELL, L. G. Visual cortical neurons: Are bars or gratings the optimal stimuli? *Science Wash. DC* 207: 88-90, 1980.
- ALLMAN, J., MIEZIN, F., AND MCGUINNESS, E. Stimulus specific responses from beyond the classical receptive field: Neurophysiological mechanisms for local-global comparisons in visual neurons. *Annu. Rev. Neurosci.* 8: 407-430, 1985.
- ALLMAN, J., MIEZIN, F., AND MCGUINNESS, E. Direction- and velocity-specific responses from beyond the classical receptive field in the middle temporal area (MT). *Perception* 14: 105-126, 1985.
- BAIZER, J. S., ROBINSON, D. L., AND DOW, B. M. Visual responses of area 18 neurons in awake, behaving monkey. *J. Neurophysiol.* 40: 1024-1037, 1977.
- BENDER, D. AND DAVIDSON, R. M. Global visual processing in the monkey superior colliculus. *Brain Res.* 381: 372-375, 1986.
- BURKHALTER, A., FELLEMAN, D. J., NEWSOME, W. T., AND VAN ESSEN, D. C. Anatomical and physiological asymmetries related to visual area V3 and VP in macaque extrastriate cortex. *Vision Res.* 26: 63-80, 1986.
- DEAN, A. F. AND TOLHURST, D. J. On the distinctness of simple and complex cells in the visual cortex of the cat. *J. Physiol. Lond.* 344: 305-325, 1983.
- DE MONASTERIO, F. M. AND SCHEIN, S. J. Spectral bandwidths of color-opponent cells of geniculocortical pathway of macaque monkeys. *J. Neurophysiol.* 47: 214-224, 1982.
- DESIMONE, R., ALBRIGHT, T. D., GROSS, C. G., AND BRUCE, C. Stimulus selective properties of inferior temporal neurons in the macaque. *J. Neurosci.* 4: 2051-2062, 1984.
- DESIMONE, R., FLEMING, J., AND GROSS, D. G. Parastriate afferents to inferior temporal cortex: An HRP study. *Brain Res.* 184: 41-55, 1980.
- DESIMONE, R. AND GROSS, C. G. Visual areas in the temporal cortex of the macaque. *Brain Res.* 178: 363-380, 1979.
- DESIMONE, R. AND SCHEIN, S. J. Receptive field properties of neurons in visual area V4 of the macaque. *Soc. Neurosci. Abstr.* 9: 153, 1983.
- DESIMONE, R., SCHEIN, S. J., MORAN, J., AND UNGERLEIDER, L. G. Contour, colour and shape analysis beyond the striate cortex. *Vision Res.* 25: 441-452, 1985.
- DE VALOIS, R. L., ALBRECHT, D. G., AND THORELL, L. G. Spatial frequency selectivity of cells in macaque visual cortex. *Vision Res.* 22: 545-559, 1982.
- DE VALOIS, R. L., YUND, E. W., AND HELPER, N. The orientation and direction selectivity of cells in macaque visual cortex. *Vision Res.* 22: 531-544, 1982.
- DEYOE, E., KNIERIM, J., SAGI, D., JULESZ, B., AND VAN ESSEN, D. Single unit responses to static and dynamic texture patterns in macaque V2 and V1 cortex. *Invest. Ophthalmol. Visual Sci.* 27, Suppl.: 18, 1986.
- DEYOE, E. A. AND VAN ESSEN, D. C. Segregation of efferent connections and receptive field properties in visual area V2 of the macaque. *Nature Lond.* 317: 58-61, 1985.
- DOW, B. M. Functional classes of cells and their laminar distribution in monkey visual cortex. *J. Neurophysiol.* 37: 927-946, 1974.
- DOW, B. M., SNYDER, A. Z., VAUTIN, R. G., AND BAUER, R. Magnification factor and receptive field size in foveal striate cortex of the monkey. *Exp. Brain Res.* 44: 213-228, 1981.
- FELLEMAN, D. J. AND VAN ESSEN, D. C. The connections of area V4 of macaque monkey extrastriate cortex. *Soc. Neurosci. Abstr.* 9: 153, 1983.
- FENSTEMACHER, S. B., OLSON, C. R., AND GROSS, C. G. Afferent connections of macaque visual areas V4 and TEO (Abstract). *Invest. Ophthalmol. Visual Sci.* 25: 213, 1984.
- FISCHER, B., BOCH, R., AND BACH, M. Stimulus versus eye movements: Comparison of neural activity in the

- striate and prelunate visual cortex (A17 and A19) of trained rhesus monkey. *Exp. Brain Res.* 43: 69-77, 1981.
24. FOSTER, K. H., GASKA, J. P., NAGLER, M., AND POLLLEN, D. A. Spatial and temporal frequency selectivity of neurones in visual cortical areas V1 and V2 of the macaque monkey. *J. Physiol. Lond.* 365: 331-363, 1985.
  25. GALLYAS, F. Silver staining of myelin by means of physical development. *Neurol. Res.* 1: 203-209, 1979.
  26. GATTASS, R., SOUSA, A. P. B., AND COVEY, E. Possible substrates for pattern recognition mechanisms. In: *Pattern Recognition Mechanisms*, edited by C. Chagas, R. Gattass, and C. Gross. Vatican City: Pontifical Acad. Sci., 1985, p. 1-20.
  27. GILBERT, C. D. Laminar differences in receptive field properties of cells in cat primary visual cortex. *J. Physiol. Lond.* 268: 391-421, 1977.
  28. GLEZER, V. D., TSHERBACH, T. A., GAUSELMAN, V. E., AND BONDARKO, V. M. Linear and non-linear properties of simple and complex receptive fields in area 17 of the cat visual cortex. *Biol. Cybern.* 37: 195-208, 1980.
  29. GROSS, C. G. AND MISHKIN, M. The neural basis of stimulus equivalence across retinal translation. In: *Lateralization in the Nervous System*, edited by S. Harned, R. Doty, J. Jaynes, L. Goldberg, and G. Krauthamer. New York: Academic, 1977, p. 109-122.
  30. GROSS, C. G., ROCHA-MIRANDA, C. E., AND BENDER, D. B. Visual properties of neurons in inferotemporal cortex of the macaque. *J. Neurophysiol.* 35: 96-111, 1972.
  31. HAMMOND, P. AND MACKAY, D. M. Differential responsiveness of simple and complex cells in cat striate cortex to visual texture. *Exp. Brain Res.* 30: 275-296, 1977.
  32. HUBEL, D. H. AND LIVINGSTONE, M. S. Complex-unoriented cells in a subregion of primate area 18. *Nature Lond.* 315: 325-327, 1985.
  33. HUBEL, D. H. AND WIESEL, T. N. Receptive fields, binocular interaction and functional architecture in the cat's visual cortex. *J. Physiol. Lond.* 160: 106-154, 1962.
  34. HUBEL, D. H. AND WIESEL, T. N. Receptive fields and functional architecture in two non-striate visual areas (18 and 19) of the cat. *J. Neurophysiol.* 28: 229-289, 1965.
  35. HUBEL, D. H. AND WIESEL, T. N. Receptive fields and functional architecture of monkey striate cortex. *J. Physiol. Lond.* 195: 215-243, 1968.
  36. HUBEL, D. H. AND WIESEL, T. N. Uniformity of monkey striate cortex: a parallel relationship between field size, scatter and magnification factor. *J. Comp. Neurol.* 158: 295-306, 1974.
  37. KRUGER, J. AND GOURAS, P. Spectral selectivity of cells and its dependence on slit length in monkey visual cortex. *J. Neurophysiol.* 43: 1055-1069, 1980.
  38. KULIKOWSKI, J. J. AND BISHOP, P. O. Linear analysis of the responses of simple cells in the cat visual cortex. *Exp. Brain Res.* 44: 386-400, 1981.
  39. LIVINGSTONE, M. S. AND HUBEL, D. H. Anatomy and physiology of a color system in the primate visual cortex. *J. Neurosci.* 4: 309-356, 1984.
  40. MAFFEI, L. AND FIORENTINI, A. The visual cortex as a spatial frequency analyzer. *Vision Res.* 13: 1255-1267, 1973.
  41. MAGUIRE, W. M. AND BAIZER, J. S. Visuotopic organization of the prelunate gyrus in rhesus monkey. *J. Neurosci.* 4: 1690-1704, 1984.
  42. MARROCCO, R. T. AND MCCLURKIN, J. W. Evidence for spatial structure in the cortical input to the monkey lateral geniculate nucleus. *Exp. Brain Res.* 59: 50-56, 1985.
  43. MICHAEL, C. R. Laminar segregation of color cells in the monkey's striate cortex. *Vision Res.* 25: 415-423, 1985.
  44. MORAN, J. AND DESIMONE, R. Selective attention gates visual processing in the extrastriate cortex. *Science Wash. DC* 229: 782-784, 1985.
  45. MORAN, J., DESIMONE, R., SCHEIN, S. J., AND MISHKIN, M. Suppression from ipsilateral visual field in area V4 of the macaque. *Soc. Neurosci. Abstr.* 9: 957, 1983.
  46. MOVSHON, J. A., THOMPSON, I. D., AND TOLHURST, D. J. Spatial summation in the receptive fields of simple cells in cat's striate cortex. *J. Physiol. Lond.* 283: 53-77, 1978.
  47. MOVSHON, J. A., THOMPSON, I. D., AND TOLHURST, D. J. Receptive field organization of complex cells in the cat's striate cortex. *J. Physiol. Lond.* 283: 79-99, 1978.
  48. PALMER, L. A. AND ROSENQUIST, A. C. Visual receptive fields of single striate cortical units projecting to the superior colliculus in the cat. *Brain Res.* 67: 27-42, 1974.
  49. PETERSEN, S. E., BAKER, J. F., AND ALLMAN, J. M. Dimensional selectivity of neurons in the dorsolateral visual area of the owl monkey. *Brain Res.* 197: 507-511, 1980.
  50. POLLLEN, D. A. AND RONNER, S. F. Visual cortical neurons as localized spatial frequency filters. *IEEE Trans. Systems, Man and Cybernetics* 13: 907-915, 1983.
  51. POGGIO, G. F., GONZALES, F., AND KRAUSE, F. Binocular correlation system in monkey visual cortex. *Soc. Neurosci. Abstr.* 11: 17, 1985.
  52. PRIBRAM, K. H., LASSONDE, M. C., AND PTITO, M. Classification of receptive field properties in cat visual cortex. *Exp. Brain Res.* 43: 119-130, 1981.
  53. RIZZOLATTI, G. AND CAMARDA, R. Influence of the presentation of remote visual stimuli on visual responses of cat area 17 and lateral suprasylvian area. *Exp. Brain Res.* 29: 107-122, 1977.
  54. SCHEIN, S. J., DESIMONE, R., AND DE MONASTERIO, F. M. Spectral properties V4 cells in macaque monkey. *Invest. Ophthalmol. Visual Sci.* 24, Suppl.: 107, 1983.
  55. SCHEIN, S. J., MARROCCO, R. T., AND DE MONASTERIO, F. M. Is there a high concentration of color-selective cells in area V4 of monkey visual cortex? *J. Neurophysiol.* 47: 193-213, 1982.
  56. SCHILLER, P. H., FINLAY, B. L., AND VOLMAN, S. F. Quantitative studies of single-cell properties in monkey striate cortex. I. Spatiotemporal organization of receptive fields. *J. Neurophysiol.* 39: 1288-1319, 1976.
  57. SCHILLER, P. H., FINLAY, B. L., AND VOLMAN, S. F. Quantitative studies of single-cell properties in monkey striate cortex. II. Orientation specificity and ocular dominance. *J. Neurophysiol.* 39: 1320-1333, 1976.
  58. SCHILLER, P. H., FINLAY, B. L., AND VOLMAN, S. F. Quantitative studies of single-cell properties in monkey striate cortex. III. Spatial frequencies. *J. Neurophysiol.* 39: 1334-1351, 1976.

59. SCHWARTZ, E. L., DESIMONE, R., ALBRIGHT, T. D., AND GROSS, C. G. Shape recognition and inferior temporal neurons. *Proc. Natl. Acad. Sci. USA* 80: 5776-5778, 1983.
60. SEACORD, L., GROSS, C. G., AND MISHKIN, M. Role of inferior temporal cortex in interhemispheric transfer. *Brain Res.* 167: 259-272, 1979.
61. SHAPLEY, R. AND LENNIE, P. Spatial frequency analysis in the visual system. *Annu. Rev. Neurosci.* 8: 547-583, 1985.
62. SHIPP, S. AND ZEKI, S. Segregation of pathways leading from area V2 to areas V4 and V5 of macaque monkey visual cortex. *Nature Lond.* 315: 322-325, 1985.
63. SPITZER, H. AND HOCHSTEIN, S. Simple- and complex-cell response dependences on stimulation parameters. *J. Neurophysiol.* 53: 1244-1265, 1985.
64. SPITZER, H. AND HOCHSTEIN, S. A complex-cell receptive-field model. *J. Neurophysiol.* 53: 1266-1286, 1985.
65. UNGERLEIDER, L. G. The corticocortical pathways for object recognition and spatial perception. In: *Pattern Recognition Mechanisms*, edited by C. Chagas, R. Gattass, and C. Gross. Vatican City: Pontifical Acad. Sci., 1985, p. 21-37.
66. UNGERLEIDER, L. G. AND DESIMONE, R. Cortical connections of visual area MT in the macaque. *J. Comp. Neurol.* 248: 190-222, 1986.
67. UNGERLEIDER, L. G., DESIMONE, R., AND MORAN, J. Asymmetry of central and peripheral field inputs from area V4 into the temporal and parietal lobes of the macaque. *Soc. Neurosci. Abstr.* 12: 1986.
68. UNGERLEIDER, L. G., GATTASS, R., SOUSA, A. P. B., AND MISHKIN, M. Projections of area V2 in the macaque. *Soc. Neurosci. Abstr.* 9: 152, 1983.
69. UNGERLEIDER, L. G. AND MISHKIN, M. Two cortical visual systems. In: *Analysis of Visual Behavior*, edited by D. J. Ingle, M. A. Goodale, and R. J. W. Mansfield. Cambridge, MA: MIT Press, 1982, p. 549-586.
70. VAN ESSEN, D. C. AND ZEKI, S. M. The topographic organization of rhesus monkey prestriate cortex. *J. Physiol. Lond.* 277: 193-226, 1978.
71. VAUTIN, R. G. AND DOW, B. M. Color cell groups in foveal striate cortex of the behaving macaque. *J. Neurophysiol.* 54: 273-292, 1985.
72. VON GRÜNAU, M. AND FROST, B. J. Double-opponent-process mechanism underlying RF-structure of directionally specific cells of cat lateral suprasylvian area. *Exp. Brain Res.* 49: 84-92, 1983.
73. ZEKI, S. M. Cortical projections from two prestriate areas in the monkey. *Brain Res.* 34: 19-35, 1971.
74. ZEKI, S. M. Colour coding in rhesus monkey prestriate cortex. *Brain Res.* 53: 422-427, 1973.
75. ZEKI, S. M. Uniformity and diversity of structure and function in rhesus monkey prestriate visual cortex. *J. Physiol. Lond.* 277: 273-290, 1978.
76. ZEKI, S. M. The representation of colours in the cerebral cortex. *Nature Lond.* 284: 412-418, 1980.
77. ZEKI, S. M. The distribution of wavelength and orientation selective cells in different areas of monkey visual cortex. *Proc. R. Soc. Lond. B Biol. Sci.* 217: 449-470, 1983.
78. ZEKI, S. M. Colour coding in the cerebral cortex: The reaction of cells in monkey visual cortex to wavelengths and colours. *Neuroscience* 9: 741-765, 1983.
79. ZEKI, S. M. Colour coding in the cerebral cortex: The responses of wavelength-selective and colour-coded cells in monkey visual cortex to changes in wavelength composition. *Neuroscience* 9: 767-781, 1983c.
80. ZUCKER, S. W. *Early orientation selection: Tangent fields and the dimensionality of their support*. Montreal, Canada: McGill Univ. Press, 1985, p. 1-33. (Dept. Elec. Eng. Tech. Rep. 85-13-R)